AD-A193 198 DEFINITION OF LONG OCEAN WAVE SLOPE FOR RADAR APPLICATIONS(U) NAVAL RESEARCH LAB WASHINGTON DC D B TRIZNA ET AL. 04 MAR 88 NRL-MR-6096 1/1

UNCLASSIFIED F/G 17/9 NL

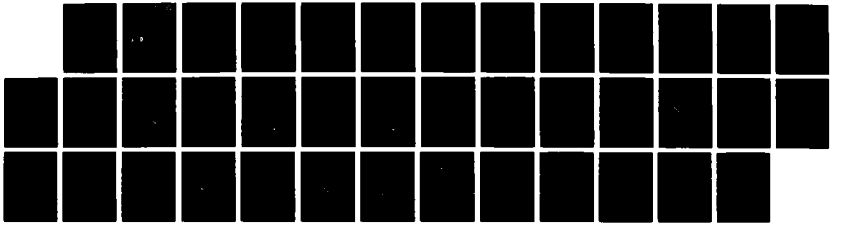

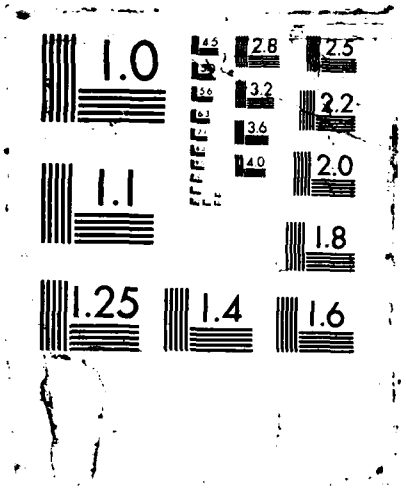
1.0
1.1
1.25
1.4
1.6
1.8
2.0
2.2
2.5
2.8
3.2
3.6
4.0
4.5
5.0

**Naval Research Laboratory**
Washington, DC 20375-5000

**NRL Memorandum Report 6096**

# Definition of Long Ocean Wave Slope for Radar Applications

DENNIS B. TRIZNA AND LEE U. MARTIN

*Radar Propagation and Scattering Staff*
*Radar Division*



March 4, 1988

SECURITY CLASSIFICATION OF THIS PAGE

## REPORT DOCUMENTATION PAGE

Form Approved
OMB No. 0704-0188

| | |
|---|---|
| 1a REPORT SECURITY CLASSIFICATION<br>UNCLASSIFIED | 1b RESTRICTIVE MARKINGS |
| 2a SECURITY CLASSIFICATION AUTHORITY | 3 DISTRIBUTION / AVAILABILITY OF REPORT<br>Approved for public release; distribution unlimited. |
| 2b DECLASSIFICATION / DOWNGRADING SCHEDULE | |
| 4 PERFORMING ORGANIZATION REPORT NUMBER(S)<br>NRL Memorandum Report 6096 | 5 MONITORING ORGANIZATION REPORT NUMBER(S) |
| 6a NAME OF PERFORMING ORGANIZATION<br>Naval Research Laboratory<br>6b OFFICE SYMBOL (If applicable)<br>Code 5303 | 7a NAME OF MONITORING ORGANIZATION |
| 6c ADDRESS (City, State, and ZIP Code)<br>Washington, DC 20375 | 7b ADDRESS (City, State, and ZIP Code) |
| 8a NAME OF FUNDING / SPONSORING ORGANIZATION<br>Office of Naval Research<br>8b OFFICE SYMBOL (If applicable)<br>ONR | 9 PROCUREMENT INSTRUMENT IDENTIFICATION NUMBER |
| 8c ADDRESS (City, State, and ZIP Code)<br>Arlington, VA 22217 | 10 SOURCE OF FUNDING NUMBERS<br>PROGRAM ELEMENT NO: 611153N<br>PROJECT NO:<br>TASK NO: RR021-05-43<br>WORK UNIT ACCESSION NO: ON280-045 |

11 TITLE (Include Security Classification)
Definition of Long Ocean Wave Slope for Radar Applications

12 PERSONAL AUTHOR(S)
Trizna, Dennis B. and Martin, Lee U.

| 13a TYPE OF REPORT | 13b TIME COVERED FROM _____ TO _____ | 14 DATE OF REPORT (Year, Month, Day) | 15 PAGE COUNT |
|---|---|---|---|
| | | 1988 March 4 | 39 |

16 SUPPLEMENTARY NOTATION

| 17 COSATI CODES | | | 18 SUBJECT TERMS (Continue on reverse if necessary and identify by block number) |
|---|---|---|---|
| FIELD | GROUP | SUB-GROUP | Remote sensing; Radar clutter; Ocean wave spectra |
| | | | |
| | | | |

19 ABSTRACT (Continue on reverse if necessary and identify by block number)

Consideration is given to the definition of open ocean long wave slope, as a parameter for correlation with radar cross section (RCS). In preparation for studies of dependence of short pulse radar statistics on long wave features, we have re-examined the long time averaged RCS data previously reported by Keller, Plant and Weissman (KPW), and its dependence on in-situ measurements of long wave slope. Comparisons of RCS are made with the significant slope defined by Huang and Long, using ocean wave spectrum features; the 'radar slope' defined in KPW, using wave spectral features inferred from radar Doppler measure of orbital wave motions; and a variety of slope definitions from zero-crossing analysis of surface variance time series measured by a wave gauge. It appears that the in-situ measurements correlate with RCS better than the 'radar slope.' Possible reasons for this are discussed.

| 20 DISTRIBUTION / AVAILABILITY OF ABSTRACT | 21 ABSTRACT SECURITY CLASSIFICATION |
|---|---|
| X UNCLASSIFIED/UNLIMITED ☐ SAME AS RPT ☐ DTIC USERS | UNCLASSIFIED |
| 22a NAME OF RESPONSIBLE INDIVIDUAL<br>Dennis B. Trizna | 22b TELEPHONE (Include Area Code)<br>202-767-2003<br>22c OFFICE SYMBOL<br>Code 5303 |

DD Form 1473, JUN 86 *Previous editions are obsolete* SECURITY CLASSIFICATION OF THIS PAGE

S/N 0102-LF-014-6603

## CONTENTS

# DEFINITION OF LONG OCEAN WAVE SLOPE FOR RADAR APPLICATIONS

## 1. INTRODUCTION

The comparison of radar backscatter cross section from a large cell size, large defined as containing several dominant ocean wavelengths, has been historically correlated with wind speed. An example of such a comparison is the series of papers by Daley and others (1968,1970,1971,1973) and Guinard, et al., (1970, 1971) using data collected with the four-frequency radar. These data were found to correlate with the only available surface truth, the wind speed measured from the aircraft. These experiments essentially formed the basis of the empirical development of radar scatterometry. The assumption forming the basis for the scatterometry technique has been that the wind excites uniformly distributed roughness elements, which form the primary Bragg scatterers responsible for the large-area averaged backscatter.

If one studies a high resolution real aperture or synthetic aperture radar image of the sea surface, one observes that the image brightness is highly correlated with the surface profile. The composite scatter model on which SAR image interpretation is based explains this behavior by assuming that the image can be represented by an average echo strength, the same large-area average measured by the scatterometer, but linearly modulated about this mean value by the large-scale surface roughness variation. This RCS intensity modulation is postulated as due to straining of the small scale Bragg-scatterer spectral density by long-wave orbital motions, and incidence angle modulation along the long wave profile. The modulation of the RCS image by the surface is assumed to be dependent to first order upon wind speed and wave frequency, and is empirically accounted for by the definition of the modulation transfer function, $m(u_*,f)$ based on the variation of the $\sigma^0$ along the wave profile (Wright, 1968):

$$\sigma^0(x,u_*) = \sigma^0(u_*)\{1 + m(u_*,f)\cos(Kx + U)\} \tag{1}$$

where $u_*$ is the wind friction velocity, $K$ is the ocean wave wave-number, $x$ is the position along the wave relative to the crest, and $U$ is the phase of the RCS peak value relative to that at the crest of the wave. Effects due to large scale surface features are generally suggested to be of second order. This model is based upon laboratory wavetank measurements for winds and paddle-generated waves of low to moderate waveheight, which are not necessarily representative of open ocean wave structures.

If this composite radar scatter model is correct, then the formalism suggests that the high resolution imagery of the surface can be used to determine the wave profile. This is so only if the modulation transfer function can be empirically defined unambiguously using a finite set of dependent variables, such as wind speed or wind friction velocity, and if effects such as long wave slope and surface contamination can be considered as of second order or lower. The detailed surface features which may be created by wave breaking are generally ignored in such a formalism.

Manuscript approved November 3, 1987.

Our interest in the statistics of marine radar scatter at low grazing angles requires a consideration of high resolution radar scatter, i.e., scatter using cell sizes with dimensions much less than dominant ocean wavelengths. Typical cell sizes for shipboard radars of interest are of the order of ten meters on a side, of the same order as SAR images but far less than the hundreds of meters for scatterometers. The normalized radar cross section (RCS) statistics for the high resolution case may contain significant contributions from just a small portion of the surface, which is either breaking or undergoing a very strong local air-sea interaction with the wind. Such contributions are generally referred to as sea spikes, and their characteristics have recently been parameterized versus wind speed (Trizna, 1987). For this case, one might expect that these statistics strongly dependent on the long wave slope, which would determine the occurrence of wave breaking as well as increase the importance of tilt modulation in the composite scatter model. Thus, the consideration of an appropriate long wave slope definition is deemed important to high resolution sea scatter studies.

In this work we compare several different definitions of long wave slope, using data previously reported upon by Keller, Plant, and Weissman (1983, hereafter referred to as KPW), collected from a research tower in the Gulf of Mexico. While the data were collected using a moderate depression angle of 45 degrees, and using vertical polarization, they are nonetheless of interest to us because of the simultaneous environmental data collected, and because of the wide range of atmospheric stability encountered. The radar data originally reported upon in KPW were twenty-one minute mean values of relative radar cross section, which were the result of an attempt to simulate a large area scatterometer cell. In preparation for this analysis, the details of the wave spectral development have been studied at some length, and are reported upon elsewhere (Martin and Trizna, 1988). In this work we concentrate on the different definitions of long wave slope, and compare them in two ways. First, each is plotted versus the mean relative radar cross section reported in KPW. We also compare the various definitions in scatter plots against the 'radar slope,' derived in KPW from Doppler shifts due to orbital wave motions. We discuss some potential problems with the radar slope definition in light of some recently reported results by Caveleri and Zecchetto (1987) on orbital wave motion distortions during conditions of high momentum transfer from winds to waves.

## II. PREVIOUS RESULTS OF KELLER, PLANT AND WEISSMAN

### 1. RCS vs Wind Speed

Figure 1 shows a subset of the RCS data reported by KPW plotted versus wind speed, the fraction of data for which sea surface variance data also were collected, and which we use here. These in-situ surface data were not utilized in KPW, but instead they used their measure of radar Doppler to determine orbital wave spectra and wave height spectra. RMS wave heights and long wave slopes were derived from these spectra and used for comparison with RCS values.

The different characters represent three different data set groupings which are discussed in a later section. The data tend to follow a curve, fitted as wind speed (U) to the 2.3 power in KPW, except for the majority of outlier points labeled with a '+' and a few diamond points. They interpreted the poor fit of these data to atmospheric stability effects. The majority of the points not used here also fit the $U^{2.3}$ curve as well. We interpret the poor fit of the outlier data to another mechanism, to be discussed elsewhere, and show this curve for comparison with later plots.

### 2. RCS vs Long Wave Slope

The definition of radar slope made in KPW used in the analysis is given by the following equation:

$$S_r(f) = (G_{vv}/a^2 C(f))[\tanh^2 Kd / \sin^2\theta \tanh^2 Kd + \cos^2\phi \cos^2\theta] \quad (2)$$

where $G_{vv}/a^2$ is the variance spectrum of line of sight orbital wave motions determined by the radar data; $C(f)$ is the phase speed of the long wave; $K$ and $f$ are its wave number and frequency; $d$ is depth; $\theta$ is the grazing angle; and $\phi$ is the angle between the antenna azimuthal pointing direction and $-K$. These results are plotted in Fig. 2, and the data points correspond to the data of Fig. 1. In addition, we have grouped all wind speeds together in this plot, rather than in 2-m/s bands as did KPW.

Because of the similar spread in RCS of Fig. 2 when compared with Fig. 1, it was decided to consider wave slope as a first order parameter for further analysis. Because it has been found that scatterometer data tends to correlate with winds best under equilibrium conditions, when pre-existing waves are not present, we considered that perhaps the long wave slope is the primary variable and that wind speed tends to correlate with RCS only implicitly, through its action in the generation of surface waves. Thus, rather than comparing RCS with wind speed and/or wind friction velocity exclusive of any consideration of the surface characterization, (currently done in the implementation of scatterometry), we decided to consider the history of the surface and wind field more closely.

## III. ANALYSIS OF WAVE DATA AND SLOPE DEFINITIONS

In Martin and Trizna, (1988), it was demonstrated that the scatter in the plot of RCS versus wind speed found in KPW was not necessarily random. That is, while a plot of all RCS vs wind speed data showed a moderate amount of scatter, plotting a temporal sequence of consecutive RCS-wind speed pairs showed a systematic track of the data with a relatively narrow scatter along that track. This suggests that a deterministic surface characterization was responsible for each individual RCS measure with little random variation from one characterization to the next. From such a result, it was concluded that the scatter in the summary plot was not random, but due to different surface characterizations. Because a given surface characterization is a result of action by the local winds plus pre-existing waves from previous winds, only under very constant winds and fully developed conditions could one expect to achieve similar surface characterizations and similar RCS values for a given wind speed. In KPW, it was found that accounting for atmospheric stability effects by plotting RCS versus wind friction velocity derived using temperature-dependent drag coefficients did not cause a narrowing of the scatter in the data. This fact lends credence to the need for further investigation of the influence of long wave slope and deterministic surface characterization on RCS variation.

Because the sequential development of the track of RCS versus wind speed was not unique, it was decided to study the development of the wave staff variance spectra with time, and to generally characterize the radar data based upon the wave spectral features and their development. These have been discussed in detail in Martin and Trizna (1988), and can be summarized as follows. Of the total data set of 22 tapes reported on in KPW, just 12 had coincident wave data with which to compare. The wind and wave data on those tapes were studied for levels of wave spectrum development, and were found to fit into one of three categories: (a) equilibrium or fully developed; (b) transient, or changing wind direction; and (c) fetch limited. These three sets are plotted in all of our figures as squares, diamonds, and plus signs, respectively.

The fetch limited data consisted of those with winds blowing between the north to northeast, off shore of the mainland some ten miles away. An analysis of tower measured winds compared with winds measured on the mainland indicated probable flow distortion effects by the tower as a cause of lower wind speeds for the off-shore, fetch-limited cases. Such effects have been previously reported by Thornthwaite, et al. (1965), on the Argus Island tower near Bermuda, and show a lowering of as much as 30% for the geometry used for the anemometer placement on the Panama City Tower. However, because of the winter-time offshore wind directions, these data were all reported with a large air-sea temperature difference as well, and they appear as outliers on the plot of Fig. 1. Flow distortion effects could account for the inability of KPW's consideration of stability effects in a wind friction velocity model to account for these outlier points. This possibility is considered further later.

## 1. Spectral Analysis

The wave data were digitized with a 0.32-s time interval, submitted to spectrum analysis using a 81.92-s integration time (0.0122 Hz resolution), and incoherently averaged over 14 spectra. This resulted in a 19.11-min averaged spectrum, from which RMS wave height and significant slope defined by Huang, Long and Bliven (1981) was determined:

$$S_{\S} = H_{rms}/L_{dom} \tag{3}$$

where $L_{dom}$ is the wavelength of the dominant wave of the spectrum, determined by the peak frequency in the spectrum, using the linear gravity wave dispersion relation, $f^2 = g/2\pi L$. Note that this definition mixes waveheight determined by all of the wave energy in the spectrum with wavelength of the longest wave of the spectrum. Hence, for waves which are not fully developed, one could expect similar significant slopes from widely different wave spectra. The results of plotting RCS versus twice this parameter is shown in Fig. 3, and clearly shows a much wider spread than do the radar slope data.

In KPW, it was reported that the radar measure of long wave slope is transparent to swell propagating off angle to the radar look direction. The small scale structure providing the radar scattering elements varies along the wind driven waves, with the swell providing only a small tilt modulation, and even that contribution cancels over the footprint of the radar for propagation directions transverse to the radar look angle. Thus, we attempted to eliminate the swell contribution to long wave slope of Eq. 3 by providing a cutoff frequency in the spectral analysis, defined by the minimum between the swell energy and the wind driven energy in the spectrum, an example shown in the plot in Fig. 4. Fig. 5 shows the result of applying this procedure to the spectrum for this slope definition. Only the spectra with significant swell contributions to the RMS waveheight are affected strongly, the triangles in the lower right hand region of the plot. The general nature of the data plotted remains the same with the swell energy eliminated.

## 2. Time Series Zero-Crossing Analysis

The 19.11-min periods of data were also submitted to analysis of the profiles of individual waves, similar to that performed by Holthuijsen and Herbers (1986). After subtracting the mean for each 19.11-min period, individual waves were defined from one down zero-crossing to the next, yielding a wave similar to that shown in Fig. 6. A linear fit to two points either side of the zero crossing was made to determine a more exact zero crossing than either of the two digitized points, thus defining the period of the wave. Parabolic fits to the regions of peaks and troughs were performed to estimate a more exact value than that of the nearest digitized point, particularly important for shorter waves. Wave periods were calculated as the time from first to the last point of the wave, using the 0.32-s time interval. Longwave lengths were determined using this period and again assuming linear gravity wave dispersion. Statistics of the wave parameters, including various definitions of long wave slope, could thus be determined for data within each 19.11-min period for comparison with RCS values reported by KPW. Note that the starting times of the 19.11-min periods were aligned with the 21-min periods used in KPW.

### i. Significant Slope Analogue from Time Series Analysis

For a high resolution radar, with cell dimension much less than the dominant ocean wavelength, a more useful slope definition than that of Eq. 2 might be one based upon local measurements of each wave. For such a definition, one must consider the time series of the wave profile. The simplest analogue to the spectral analysis result of Equation 1 would be the local measure of the ratio of trough-to-peak height to trough-to-peak distance. Using such a method, a ratio equivalent to Eq. 3 can

be calculated for each wave beginning at a zero down crossing as is shown in Fig. 1, for example, and the median value taken of the resultant distribution of slopes:

$$S_{H/L} = <2H_j/L_j> \tag{4}$$

where $< >$ indicates averaging over all individual waves within the time period, and $Lj$ is the total wave length from one down zerocrossing to the next, across $N$ time samples:

$$L_j = C(f)(t_n - t_1) \tag{5}$$

Note again that the ratio of full height to half wavelength was used, to define a true measure of slope, introducing the additional factor of 2 relative to Eq. 2. These results are shown in Fig. 7. Using this definition, one is assuming that all waves are sinusoidal, with no account taken for profile asymmetry.

While scaling somewhat differently in magnitude, these data appear similar to the $S_r$ plot, except for some of the transient data, which lie above the generally tight cluster. These particular points occurred just after the 180-deg change in wind direction, with surface roughness generation not in equilibrium with the wind. In fact, the fit of RCS to $S_r$ for these data is probably due to orbital wave motions of waves travelling away from the radar rather than toward it, as is usually assumed to be the case for waves in equilibrium with the wind. The method of calculation of orbital wave spectra cannot distinguish between approaching and receding waves. Note that except for these outlier data, the fit of RCS vs $S_{h/L}$ is actually tighter than that vs $S_r$. it is clear that the two techniques are measuring a quite different slope for the transient data, a point which we shall return to later.

ii. Slope of an Asymmetric Profile — Upper Half Forward Face

The waves were found to be asymmetric in shape, similar to results found by Holthuijsen and Herbers (1986). Because one might expect stronger scatter from steep waves, either due to breaking features associated with the steepest crests, or tile modulation and enhanced small scale structure on the forward face of the steepest waves, it was decided to extend the definition of long-wave steepness to include this asymmetry as well.

In their study of the dependence of breaking waves on forward face wave steepness, using the asymmetric wave of Fig. 6, Holthuijsen and Herbers (7) defined the slope of the upper-half forward face of the wave according to the following equation:

$$S_{A1} = <A1_j/L1_j> \tag{6}$$

which scales in a similar fashion to the earlier definitions. These results appear in Fig. 8, and show less scatter than the previous fit, indicating a better correlation, again discounting the outlier data corresponding to the transient data. The slopes are found to be steeper that the previous plot for the highest RCS region, as expected due to the asymmetry, but very similar for the low RCS values. This indicates that the low RCS region probably is very close to sinusoidal in wave profile.

iii. Slope of an Asymmetric Profile — Full Forward Face

While the upper-half wave slope may be useful for correlation with wave breaking because it is the steepest portion of the wave, one might expect enhanced radar scatter from the entire front face of the wave. An equivalent definition to $S_{A1}$ can be made for the peak-to-trough height over the distance along the wave between these points:

$$S_{A2} = <H_j/(L_1 + L_4)> \tag{7}$$

These results are shown in Fig. 9, and appear similar to the $S_{A1}$ data, but with some of the transient data near 0.16 to 0.18 showing a somewhat smoother variation. This plot may be considered as best correlated with RCS of slope definitions so far, again discounting the one set of transient data. If one plots $S_{A1}$ vs $S_{A2}$ as shown in Fig. 10 with a unit-slope line super-imposed, one sees very little scatter except for the fetch-limited data at the high end, and indicating steeper upper half profiles, and perhaps wave breaking.

iv. Median Local Slopes

In each of the following definitions, the lengths along the wave are determined by measuring the slope between adjacent digitized time samples, similar to the definition of Eq. 5:

$$dL_j = C(f)dt_j \tag{8}$$

where $j$ now indicates the $j$th sample of the wave profile. The long wave profile defines the phase velocity again.

The first of these slope definitions to consider is that defined by the point to point incremental height increases, $dH_j$, over $dL_j$ across the upper half of the forward face (*uhff*) of the wave:

$$S_{Loc1} = <dH_j/dL_j>_{uhff} \tag{9}$$

where $<>$ and *uhff* indicates a median over all samples on the upper-half forward face of a 19.11-min time series. As an analogue to Equation 4, one could also consider the full forward face (*fff*):

$$S_{Loc2} = <dH_j/dL_j>_{fff} \tag{10}$$

Finally, one could make an equivalent definition over the full wave period, but taking the absolute magnitude of $dH_j$, so as to avoid a zero mean slope over the wave period:

$$S_{Loc3} = <|dH_j|/dL_j> \tag{11}$$

The results for these three definitions are shown in Figs. 11, 12 and 13, respectively. The plots of RCS vs $S_{loc1}$ and $S_{loc2}$ show a similar behavior, with wide scatter for the transient data and some of the fetch limited data. This may be due to small scale structure, of the order of 0.32-s scale size riding on the longer waves. A small sinusoid riding on a large wave defined by zero crossings could add negative slope contribution to the sum used to generate $S_{loc1}$ and $S_{loc2}$, accounting for this added scatter. One may only speculate as to whether or not this implies small scale breaking. The correlation of all local slopes with RCS is not as good as that of $S_{A2}$.

v. Radar Slope

Keller, et al., calculated the "radar slope," based upon assumptions that the time history of the measured radar Doppler shift is determined by the orbital wave motions of the scattering cell, and that these waves are purely linear. Given the depression angle of the radar, the orbital wave motion spectrum can be determined, which is the time derivative of the wave profile. The slope definition made by KPW for comparison with the time averaged relative radar cross section is the following:

$$SS_r = [K_{dom}^2 \int S_r^2 df]^{1/2} \tag{12}$$

where $\int (S_r)^2 df$ is the integral of the slope variance spectrum of Eq. 2. This definition is analogous to that of Huang, Long and Bliven. We shall consider some of the problems associated with the assumptions made in conjunction with this definition later.

## IV. CORRELATION OF RADAR SLOPES AGAINST OTHERS

In order to identify the slope definition with which the radar slope best correlates, we plotted $S_r$ against all of the time-series definitions, having eliminated the significant slope definition made from the spectral analysis because of the generally poor correlation with RCS values shown earlier.

The first of the definitions to be compared is $S_{H/L}$, shown in Fig. 14, with a unit-slope line superimposed indicating perfect correlation. The $S_{H/L}$ values were found earlier to be generally higher than the $S_r$ values, but a new fact emerges from this plot: the clustering of data according to our earlier definition of three classes of wind wave systems. The fetch-limited data cluster higher than the mean in a region, the transient data cluster lower, and the equilibrium values tend to cluster in the middle. While the $S_{H/L}$ definition is the closest to a Fourier component using this type of analysis, the wave height used in its definition does include higher order Stokes wave harmonic contributions. The radar slope technique measures the Fourier component, with no such harmonic contributions. Hence, perhaps it is not surprising that such clustering occurs for this comparison. One might expect such clustering for the rest of the time series definitions as well, because in addition to using the same height as $S_{H/L}$, they also include asymmetry features which the Stokes wave does not include. This clustering thus indicates that for slopes measured as similar in magnitude by the radar slope technique, the in-situ measurement distinguishes between the three types of wave systems.

Figure 15 shows the $S_{A1}$ comparison, with a straight line of unit slope again. The results are similar to the last plot in the distribution of the data points in the separation according to three types. However, now all in-situ values are higher than larger than the radar measure, due to the asymmetry discussed above.

To compare the two in-situ sets more closely, the correlation of $S_{A1}$ against $S_{H/L}$ is shown in Fig. 16, both with a unit slope and a least squares fit. $S_{A1}$ is seen to be roughly 7% steeper than the symmetric Stokes wave approximation, but very little departure from the linear variation occurs over the entire range of slope values. This implies asymmetry scales linearly with Stokes wave steepness. Finally, plots of radar slope versus the two local slopes in Figs. 17 and 18 show even worse scatter than the last two cases, as might have been expected from results of the last section.

## V. LONG WAVE SLOPES vs CORRECTED WIND SPEED

As a final item, we compare the radar slope and the $S_{A2}$ definition of long wave slope with wind speed. However, now we are confronted with the proper correction factor to use, to deal with the wind directions for which flow distortion effects may be important. For these comparisons, to test for assumed wind speed error measurements of 30%, 20%, 10%, and 0% due to flow distortion effects to the platform, we have divided all wind speeds for northerly directions by 0.7, 0.8, 0.9, and 1.0 for the four cases, shown for the radar slope in Figs. 19 a-d. The data which are shifted include the four fetch-limited cases, #'s 41, 42, 44, 45, and the first tape of the transient group, #22. For this transient case, the highest winds occur just after the direction change, then slowly decrease in magnitude. Results from a similar analysis applied to the $S_{A2}$ data are shown in Figs. 20a-d.

If one assumes the worst flow distortion effects, and the strongest correction of 30% applied to the radar slope, the result is shown in Fig. 19a. All of the fetch limited data fall within the bounds of the equilibrium and most transient data, and a straight line with slope 0.015 and zero intercept provides a reasonably accurate fit. The early transient data of tape #22 fall far to the right of the data

cluster. Because these data were collected during winds blowing against waves from the opposite direction, generated earlier, one should not expect the orbital wave motions to be associated with local winds. On the other hand, the Fourier component of the long wave slope could be expected to be similar for the remainder of the data, and show no difference according to our three types of waves. For no flow distortion correction, Fig. 19d, the early transient data lies in general agreement with the rest of the data, while the fetch limited sets spread above the rest. This is probably an incorrect result for reasons discussed above. For corrections of 10% and 20%, the data lie in between these two cases.

The same corrections were applied to the $S_{A2}$ definitions, shown in Figs. 20 a-d. For 20a, a straight line with slope of 0.020 and zero intercept provides a reasonable fit. Similar results occur for the $S_{A2}$ slopes as for the radar slopes. However, now the data remain slightly separated for the tape #22 data even for 30% correction. Note also that the $S_{A2}$ slopes for these data are not among the highest of the set as they were for the radar slope. One would expect these preexisting waves to be suppressed in front-face slope immediately after the wind shift, because the winds are beating these wave down, thus accounting for these results.

## VI. RCS vs CORRECTED WIND SPEED

In similar fashion to the previous section, one can plot the mean RCS of KPW against the wind speed corrected for flow distortion effects. Figures 21a-d show the results for the same corrections applied in Figs. 19 and 20. For the largest correction, the fetch limited points have been shifted closer to the main body of the data, and those for tape #22 have been shifted far to the right of the main body. Because these latter transient points are for times for which the waves are not yet in equilibrium with the waves, the RCS are not yet to their corresponding value expected for that wind speed. The data labeled as fetch limited still exhibit larger RCS values than expected for the corresponding wind speeds.

Because the plots of RCS vs $S_{A2}$ plotted earlier show a smooth variation with increasing slope, we conclude that the long wave slope is a more realistic parameter against which to compare than wind speed. Thus, we interpret the current discrepancy in Fig. 21a as due to the fact that the wave slope, $S_{A2}$, correlates with wind speed differently for limited fetch than for unlimited fetch. Thus, as long as the wind is blowing in the same direction as the waves, i.e., a recent change in wind direction has not occurred, the RCS will correlate with long wave slope, $S_{A2}$, whether or not the waves are fully developed. On the other hand, RCS will correlate with wind speed only if waves are fully developed, but not if the waves are fetch limited or winds are transient.

## VII. DISCUSSION

(i) General Conclusions

One can draw the following conclusions from this analysis.

(1) First, the significant slope of Huang and Long has little meaning in the context of radar scatter, except perhaps for equilibrium conditions without swell. Even for such conditions, the slope so-defined scales much differently than radar slope or any of the in-situ slope definitions. It is not clear why there should be such a great difference from the radar slope data, because they were formally defined in a similar manner.

(2) Second, it appears that the radar slope, $SS_r$, measures something quite different than the in-situ definitions. A plot of RCS vs all of the in-situ definitions shows a clustering according to

different groupings of the wave data, indicating a parameterization according to local steepness, and perhaps wave profile asymmetry and occurrence of wave packets, as well as other characterizations associated with these groupings. How ever, no such clustering occurs with the radar slope definition. Instead, the radar slope data show a relatively broad spread plotted vs RCS, whereas the in-situ definitions show a definitely narrower spread within each cluster.

The radar slope measures just a Fourier component of the long wave slope, which cannot account for the non-linear steepening of waves and the asymmetric departure from a sinusoidal profile. One might expect a difference to occur when comparing with slope definitions which account for such non-linearities. Such a grouping occurs for comparisons with $S_{H/L}$, the simplest of our in-situ definitions, which takes into account the higher harmonic amplitude contributions to the wave but no asymmetry. Accounting for wave asymmetry using $S_{A1}$ and $S_{A2}$ creates larger wave slopes, and the data continue to cluster.

One might ask what effects the occurrence of wave packets have on the application of Fourier analysis techniques, in addition to those of non-linear, asymmetric waves. In particular, if one uses coherent integration times which are longer than the coherence time of a packet, i.e., times enveloping several wave packets, then the energy from these packets can add out of phase, because the relative phases between adjacent wave packets is expected to be a random variable. Such effects would play a role in both the determination of orbital motion spectra using Doppler techniques, as well as height-variance spectral analysis. To the authors' knowledge, such effects have not be investigated.

(3) Third, because of the relatively broad spread of RCS plotted against radar slope, it appears that radar slope is not a significant parameter for RCS correlation as it stands. Because of the clustering by the three types of data defined (transient, equilibrium, and fetch limited) on the plots of RCS vs several definitions of in-situ slope, it appears that local wave slope plays a large part in determining RCS, whether it be due to stronger tilt modulation or the occurrence of breaking features. Furthermore, it appears that these slopes can be used to parameterize against RCS, particularly $S_{A2}$. First, however, an understanding of the reasons for the clustering of these three groups is required. More information about the state of development of the wave system is needed, which further details of the profile shape may provide, perhaps a measure of asymmetry such as the ratio, $L_1/L_2$, of Fig. 4 or a measure of wave packet coherence lengths. Work is progressing in this area currently.

(4) Because of a similar scatter of RCS vs wind speed for the three types of data, it appears that wind speed is alone a poorer quantity against which to correlate RCS than in-situ long wave slope, until one understands the cause of the clustering.

(5) In the plots of RCS vs all in-situ defined slopes, a small set of transient data points which lay above the rest of the data were for the case of winds just having turned 180 deg. One might surmise that this case of winds blowing into opposing waves could have created breaking or some type of fluid separation which gave an unusually high RCS for the a relatively small local local long wave slope. These data also were outlier points on the original RCS-wind speed plot of KPW, and were unexplained. It follows that such occurrences of rapid wind direction changes might thus be expected to create problems for scatterometry as well.

We conclude that we have identified a correlation of in-situ measurements of local slope with RCS which differs according to the three groupings of surface development which we have used. These may be important in particular for studies of the influence of wave breaking on radar scatter statistics, our original aim.

(ii) Importance to Scatterometry

With this perspective of long wave slope as an independent parameter in correlation with RCS, one can comment on the success or lack thereof of empirical scatterometer models. The success of scatterometer data comparisons can perhaps be explained by the high percentage of time the winds and waves are in equilibrium on occasions when such measurements have been made. The large scatter in the RCS-wind speed data bases used to derive scatterometer algorithms may be due in part to the effect of non-equilibrium characterizations of the local surface, particularly the occurrence of swell and pre-existing wave systems, i.e., generally confused seas. The data considered here do not purport to satisfy a realistic percentage of occurrence of the three types chosen. Nevertheless, we suggest that the particular characterization of the sea surface is significant in influencing RCS measures, and that wind speed or wind stress alone may only be implicitly responsible, via its generation of the wave system.

(iii) Radar-Derived Slope Errors

One error to be expected in definition of radar slope is that due to non-sinusoidal wave profiles, and hence, non-circular orbital wave motions of surface water particles. A realistic approximation to the non-sinusoid is the Stokes wave, with a series of harmonics traveling at the same phase velocity as the fundamental. However, since the orbital wave speed periodicity of the first harmonic is twice that of the fundamental, the contribution to the orbital wave spectrum is at twice the frequency of the fundamental. Hence, for a Stokes profile, the higher order contributions occur at different wave frequencies and the orbital wave estimate of the wave height is just that of the fundamental. However, this is also true of spectral analysis of the same ocean waves measured by a buoy time series. The long non-linear ocean wave is underestimated by spectral analysis, yielding only the linear component's contribution to the wave profile. Thus, the radar slope is underestimating the true local slope in all cases for which the waves depart significantly from non-linear theory, which may be important for occurrence of wave breaking.

Finally, one must consider recent results on the nonclassical behavior of the orbital motions of ocean waves under conditions extremely high wind stress and wave breaking reported recently by Cavaleri and Zechetto (1987). Their measurement of the trajectories of water particles below the surface indicated that for cases of large momentum flux from the atmosphere to the water, the particle motions were elliptical as expected, but with the ellipse axis tilted downward in the direction of the wind. In plotting wind stress versus wave height, they found a 2.27 exponent for H rather than 2 expected for linear waves, indicating strong non-linear processes occurring, probably wave breaking. This tilting angle was to be a function of water wavelength, the greater tilt occurring for longer wavelengths. Such as axis tilt may have a similar effect on the Doppler measurements of the surface motions used to deduce radar slope discussed herein.

The authors wish to acknowledge the discussions with Professor Jin Wu, of the University of Delaware, who suggested the local slope characterization, which ultimately lead to the parameterization according to Holthuijsen and Herbers. We also wish to acknowledge the efforts of John Fahnestock in developing the software which allowed comparison of the various data sets.

## REFERENCES


1. Cavaleri, L. and S. Zecchetto, "Reynolds Stresses Under Wind Waves," JGR, Vol. 92, NC 4, pp. 3894-3904, 1987.

2. Daley, J.C., J.T. Ransone, J.A. Burkett, and J.R. Duncan, "Sea Clutter Measurements on Four Frequencies," NRL Report 6806, Naval Research Laboratory, Washington, D.C., 1968. - AD 850069L

3. Daley, J.C., W,T. Davis, and N.R. Mills, "Radar Sea Return in High Sea States," NRL Report 7142, Naval Research Laboratory, Washington, D.C., 1970. - AD 713589

4. Daley, J.C., J.T. Ransone, and J.A. Burkett, "Radar Sea Return — JOSS I," NRL Report 7268, Naval Research Laboratory, Washington, D.C., 1971. - AD 725110

5. Daley, J.C., J.T. Ransone, and W.T. Davis, "Radar Sea Return — JOSS II," NRL Report 7534, Naval Research Laboratory, Washington, D.C., 1973. - AD 757655

6. Guinard, N.W. and J.C. Daley, "An Experimental Study of a Sea Clutter Model," Proceedings of the IEEE, Vol. 58, pp. 543-550, 1970.

7. Guinard, N.W., J.T. Ransone, and J.C. Daley, "Variation of the NRCS of the Sea with Increasing Roughness," JGR, Vol. 76, pp. 1525-1538, 1971.

8. Holthuijsen,L.H., and T.H.C. Herbers, "Statistics of Breaking Waves Observed as Whitecaps in the Open Sea," J. Phys. Ocean., Vol. 16, pp. 290-297, 1986.

9. Huang, N.E., S.R. Long, and L.F. Bliven, "On the Importance of the Significant Slope in Empirical Wind Wave Studies," J. Physical Oceanography, Vol. 11, pp. 569-573, 1981.

10. Keller, W.C., W.J. Plant, and D.E. Weissman, "The Dependence of X Band Microwave Sea Return on Atmospheric Stability and Sea State," JGR, Vol. 90, pp. 1019-1029, 1985.

11. Martin, L.U. and D.B. Trizna, "Analysis of Environmental Data From the 1978 Panama City Tower Radar Experiment," NRL Memo Report 6100, 1988.

12. Thornthwaite, C.W., W.J. Superior, and R.T. Field, "Disturbance of Airflow Around Argus Island Tower Near Bermuda" JGR, Vol. 70, pp. 6047-6052, 1965.

13. Trizna, D.B., "Measurement and Interpretation of North Atlantic Ocean Marine Radar Sea Scatter," NRL Report 9099, 1988.

14. Wright, J.W., "A New Model for Sea Clutter," IEEE Trans AP-14, pp. 217-223, 1968.

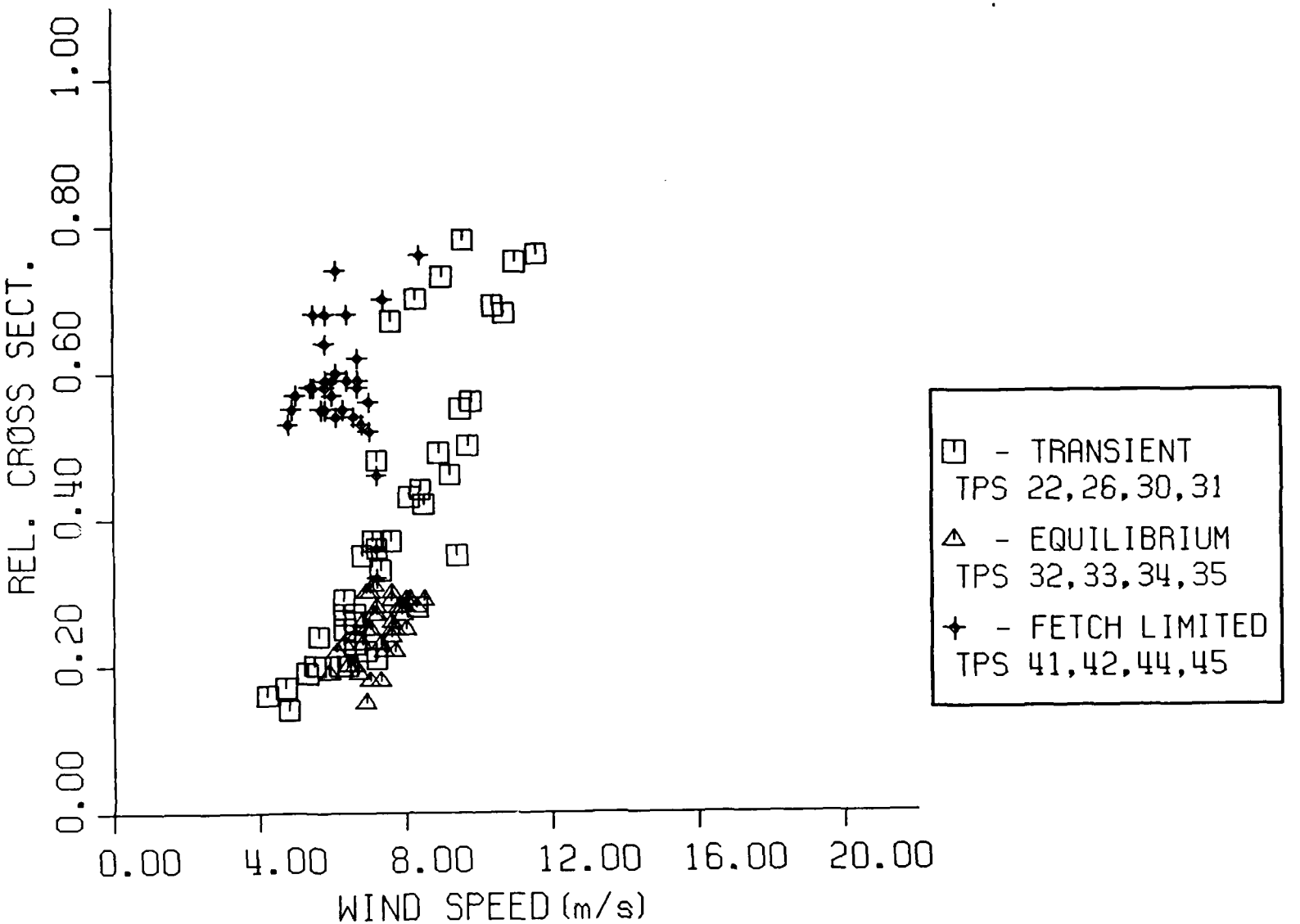


Fig. 1 — A subset of the plot of RCS vs wind speed reported by Keller, Plant, and Weissman, for which wave staff records were collected

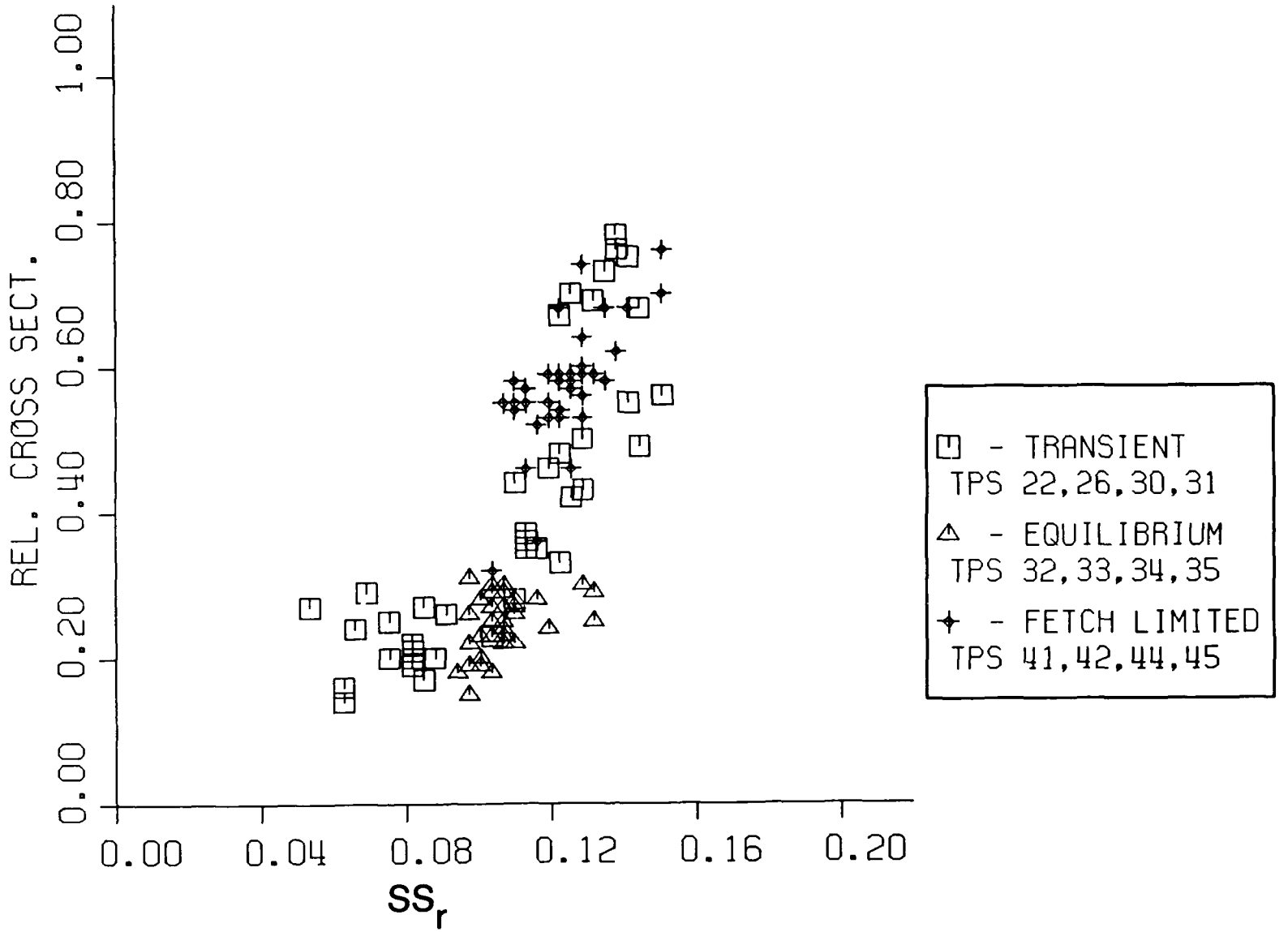


Fig. 2 — A plot of RCS vs radar slope is shown for the same subset described in Fig. 1

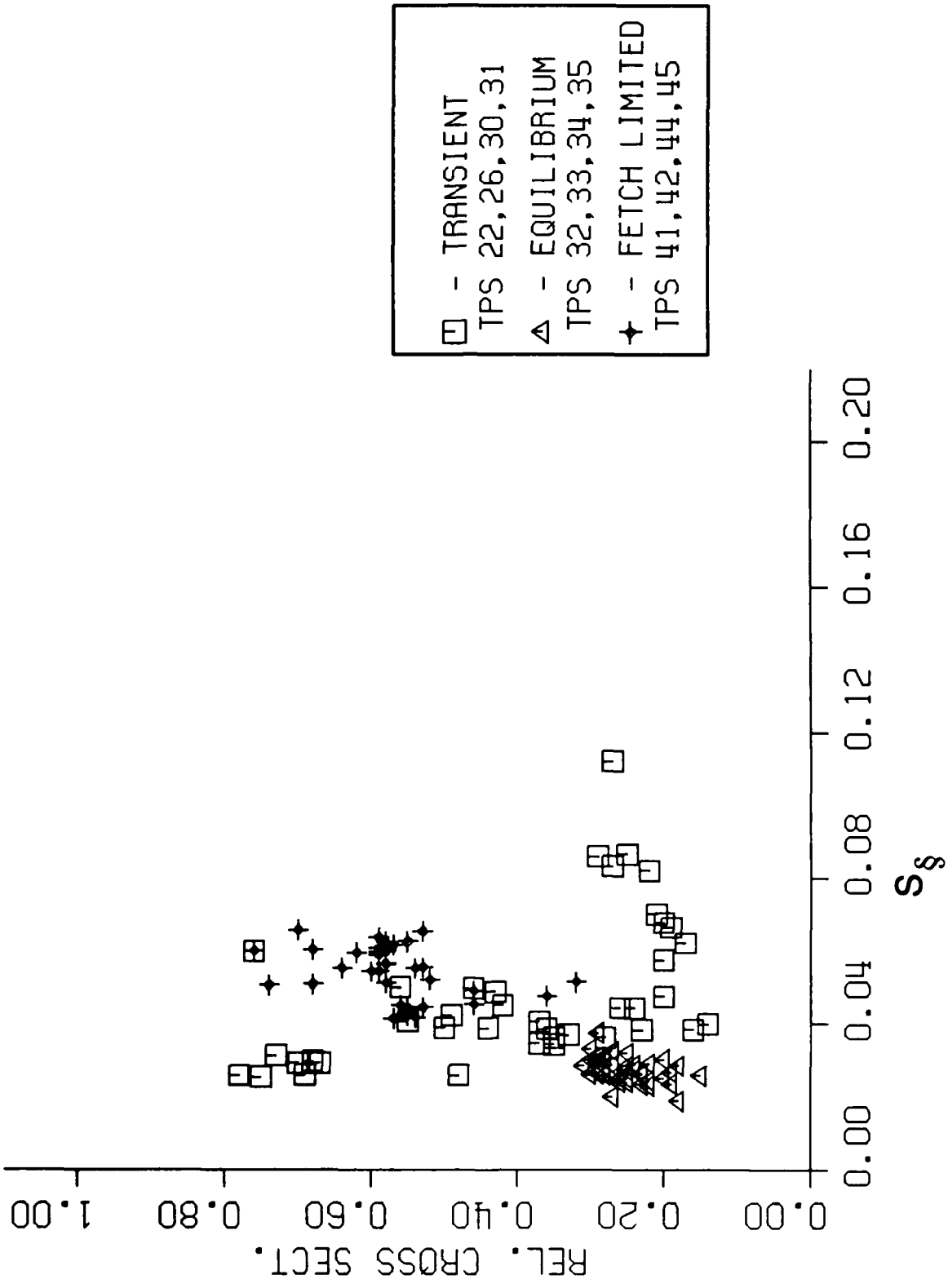


Fig. 3 — A plot of RCS vs $S_{Spec}$, the significant slope definition of Huang and Long, using wave spectrum data

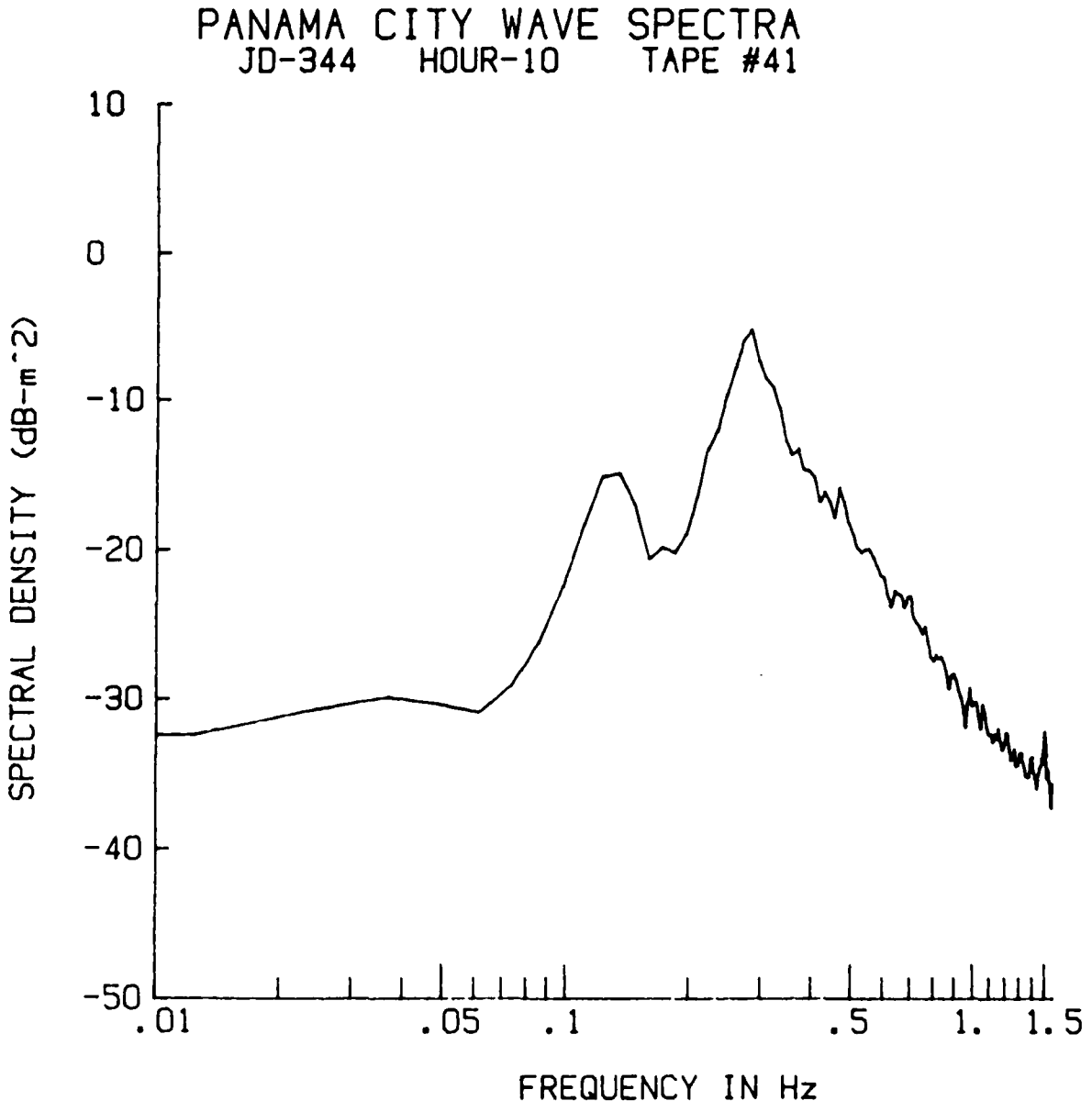


Fig. 4 — An example of a wave spectrum which contained significant swell energy, which was eliminated for the modified definition of significant slope

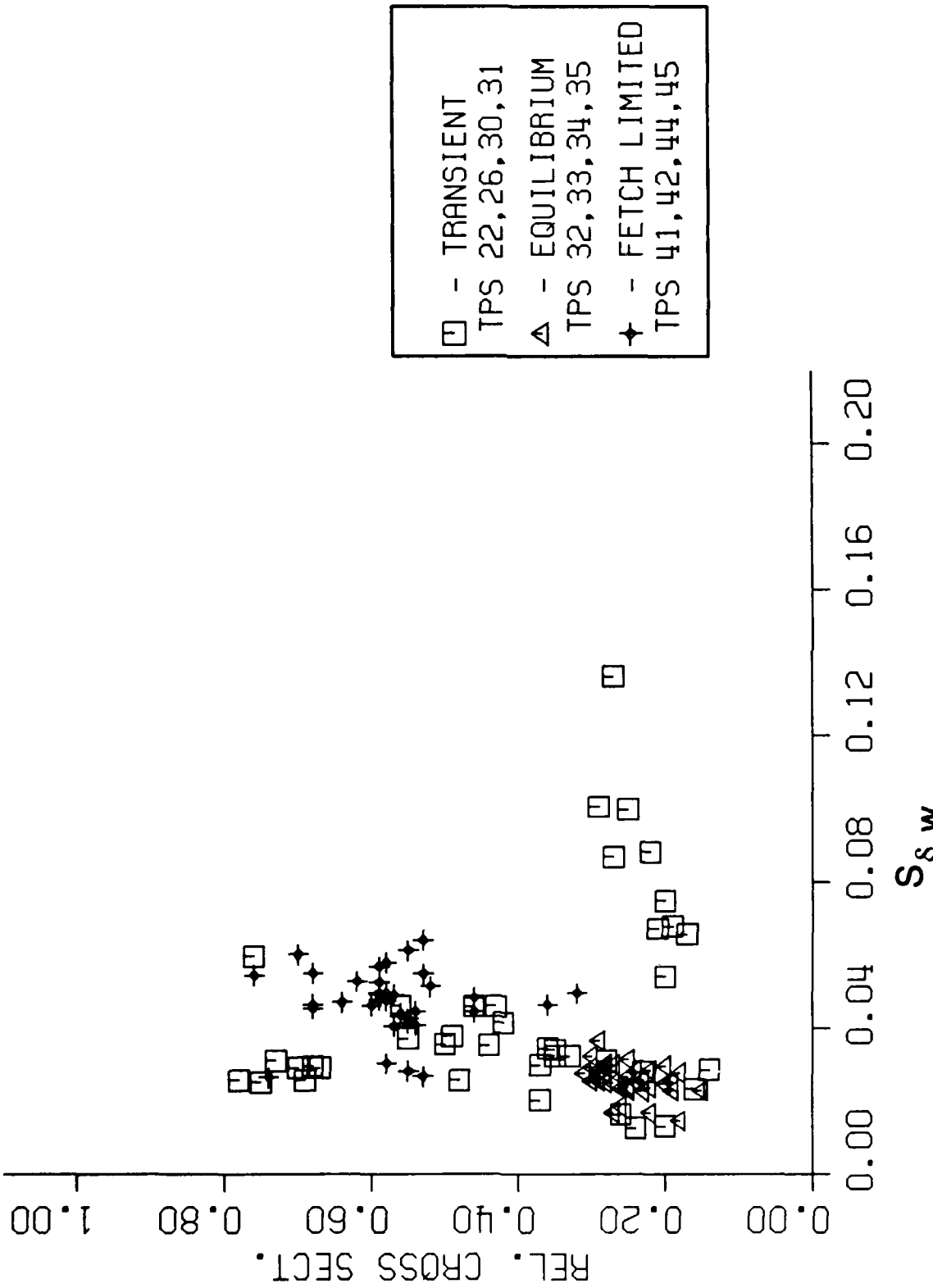


Fig. 5 — A plot similar to those of Fig. 3, but for swell removed for the significant slope definition

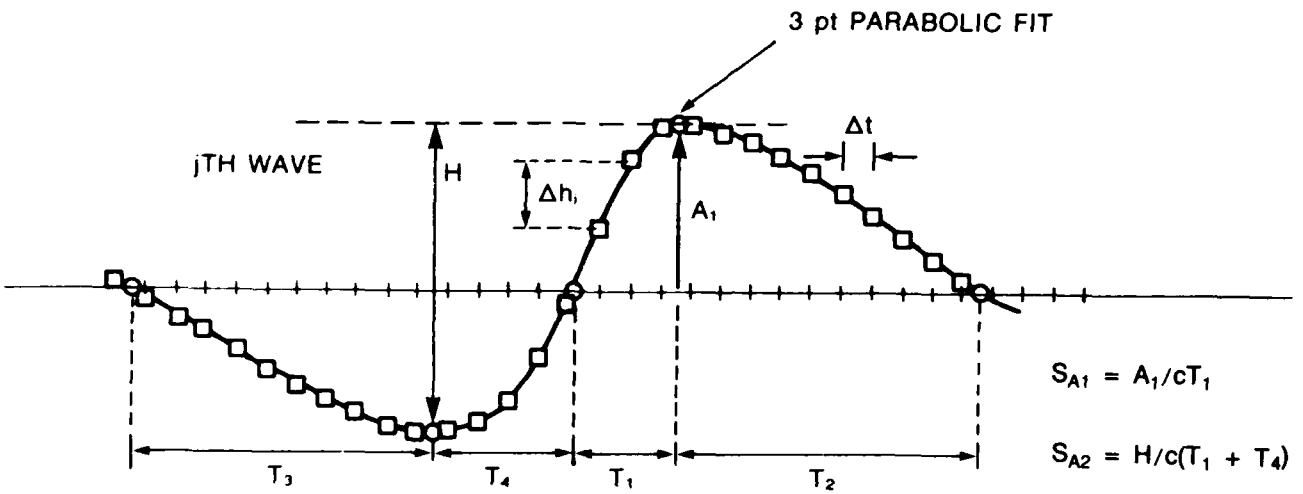


$$T = T_1 + T_2 + T_3 + T_4$$

$$C = \Omega/K = gT/2\pi$$

$$L = cT$$

$$S_{A1} = A_1/cT_1$$

$$S_{A2} = H/c(T_1 + T_4)$$

$$S_{H/L} = 1/2\, H/cT$$

$$S_{loc1} = \frac{1}{N}\sum_{j=1}^{N} \Delta h_i/c\,\Delta t_i\,\Delta t_i \in T_1,$$

$$S_{loc2} = \frac{1}{N}\sum_{j=1}^{N} \Delta h_i/c\,\Delta t_i\,\Delta t_i \in (T_1 + T_4)_i$$

$$S_{loc3} = \frac{1}{N}\sum_{j=1}^{N} |\Delta h_i|/c\,\Delta t_i\,\Delta t_i \in T_i$$

Fig. 6 — An example of the various slope definitions considered in the text are shown graphically for a steep, asymmetric wave profile

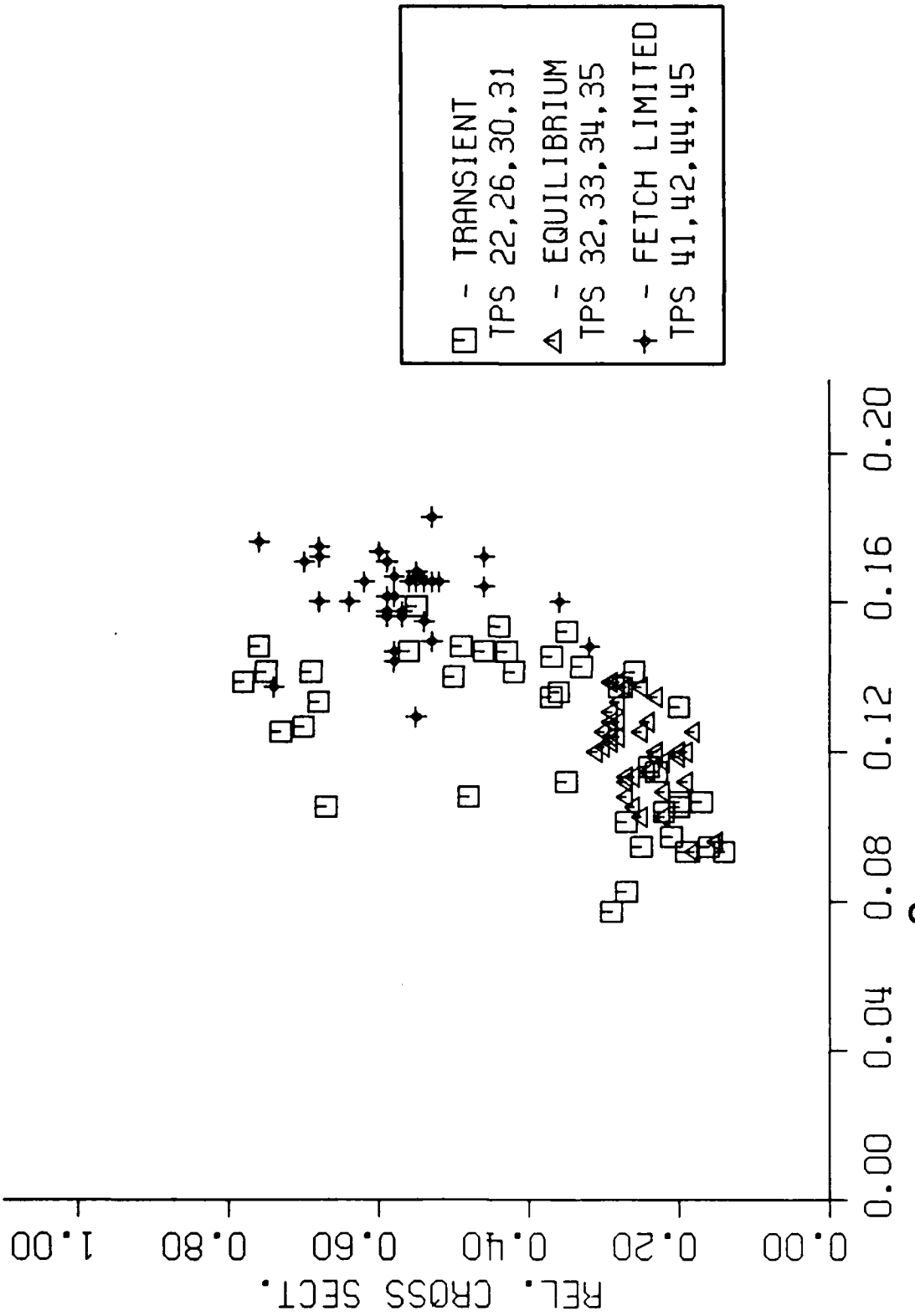


Fig. 7 — A plot of RCS vs $S_{H/L}$ defined in Eq. 4 is shown

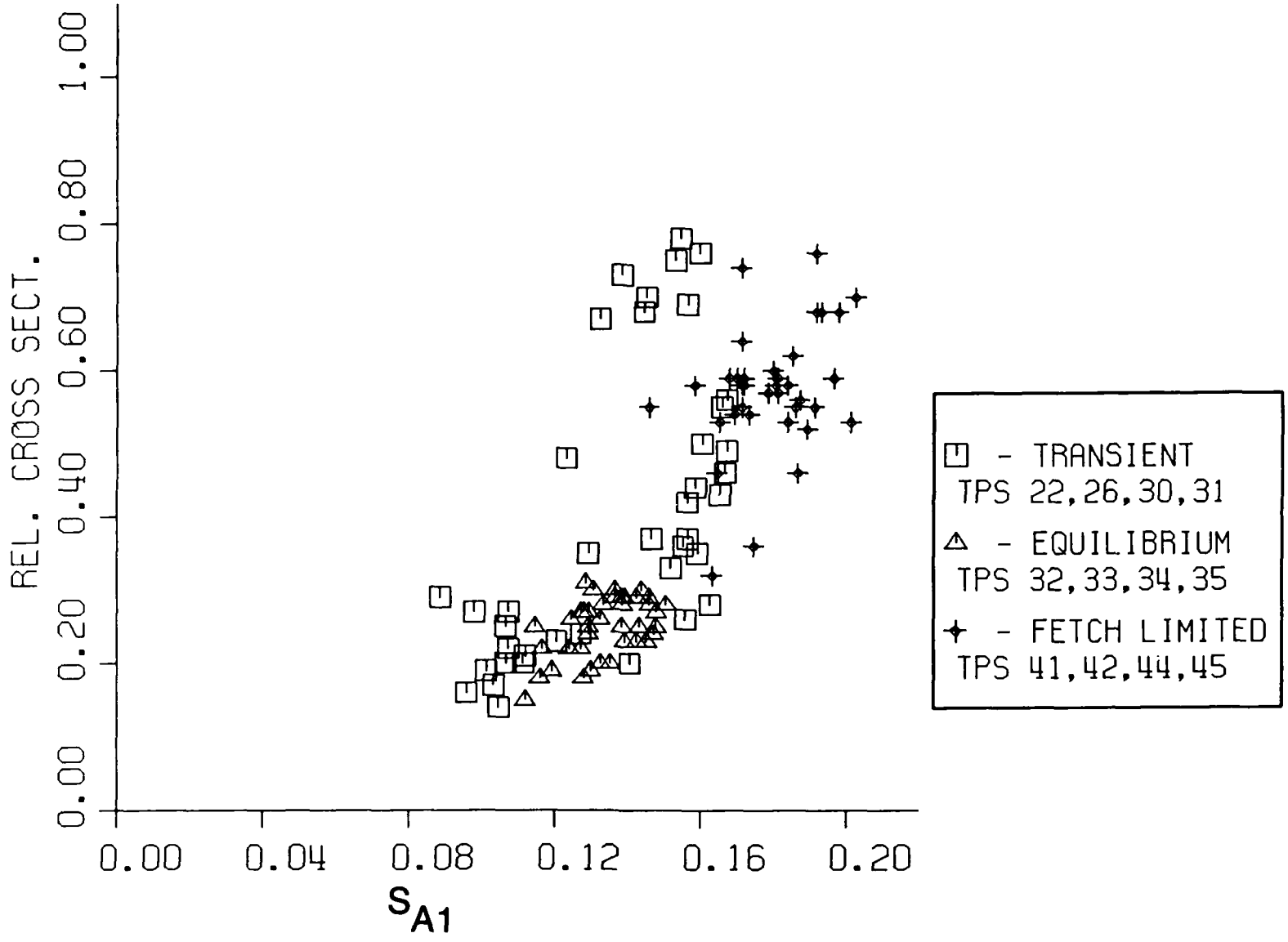


Fig. 8 — A plot of RCS vs $S_{A1}$ defined in Eq. 6 is shown

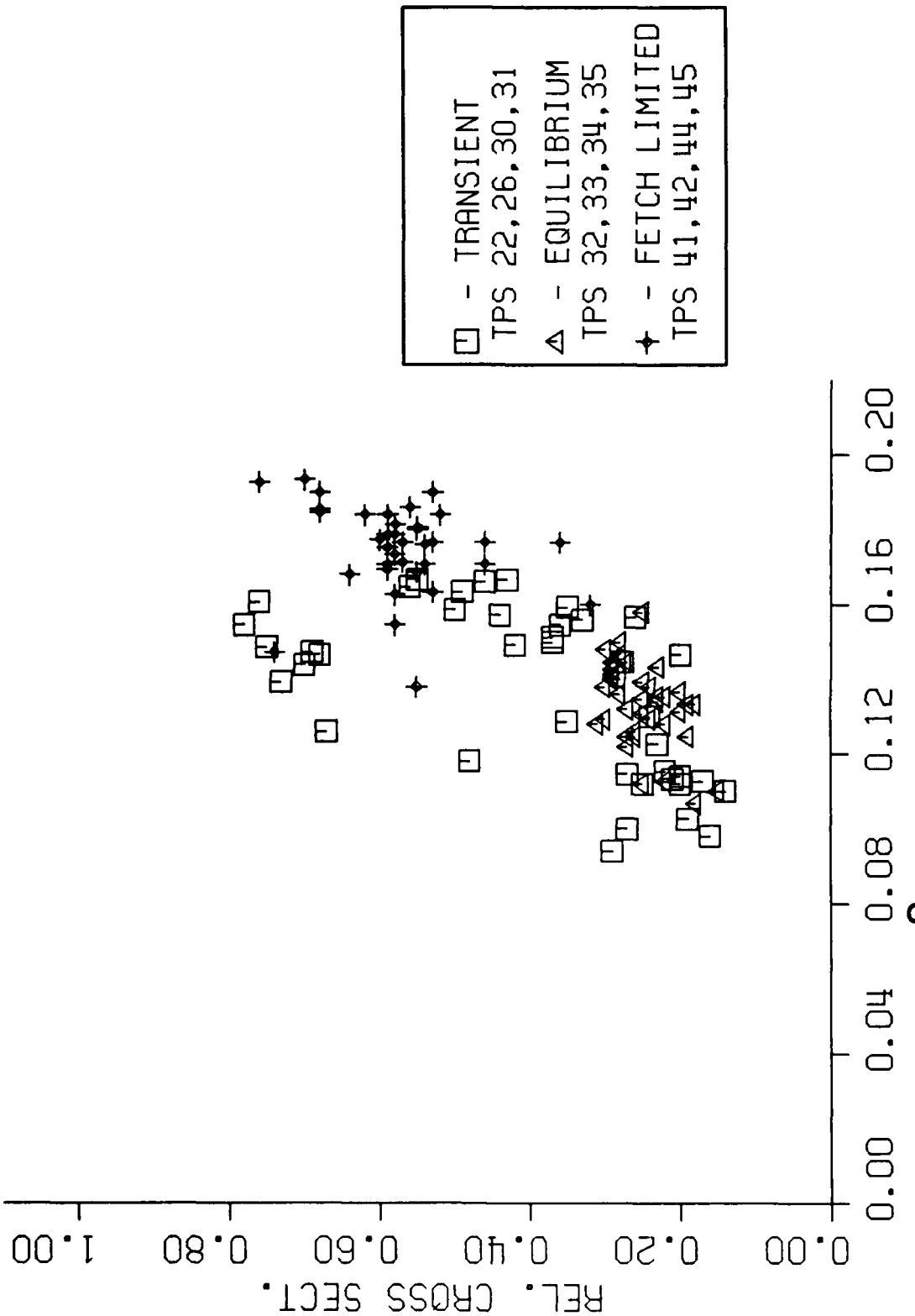


Fig. 9 — A plot of RCS vs $S_{A2}$ defined in Eq. 7 is shown

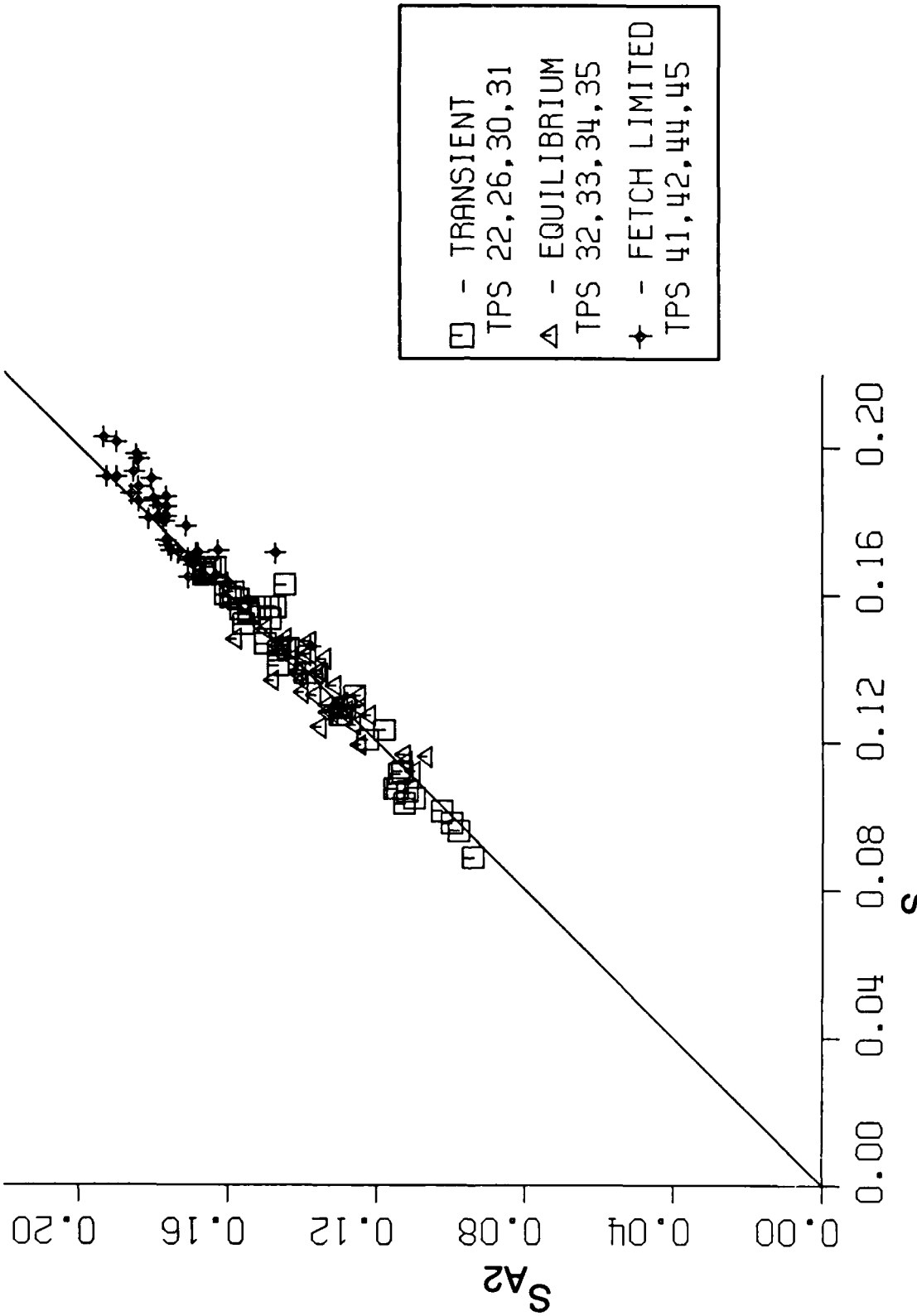


Fig. 10 — A scatter plot of $S_{A1}$ vs $S_{A2}$ is shown, indicating the lower half of the forward face of the wave has roughly the same slope as that of the upper half for these data

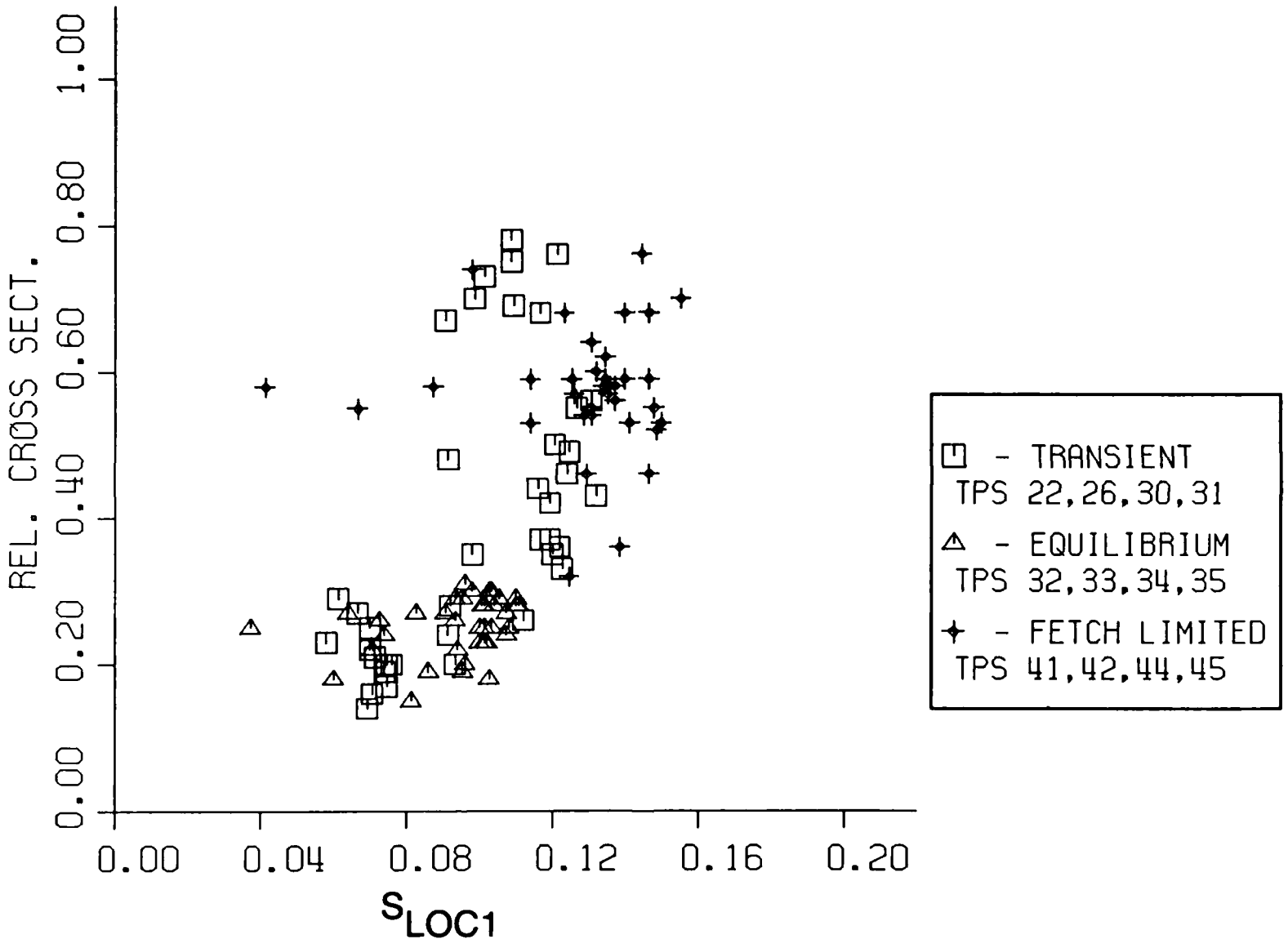


Fig. 11 — A plot of RCS vs $S_{loc1}$ defined in Eq. 9 is shown

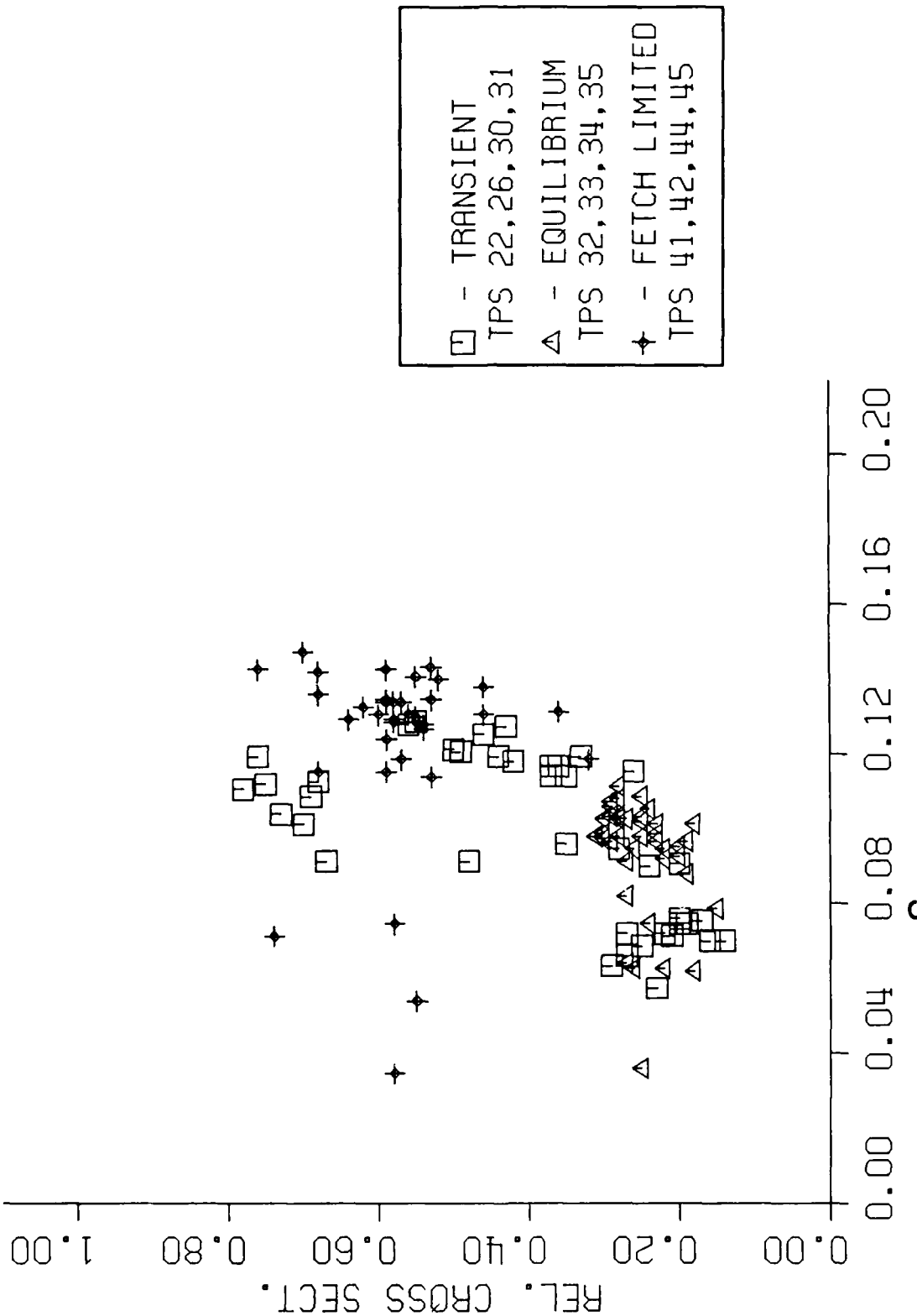


Fig. 12 – A plot of RCS vs $S_{loc2}$ defined in Eq. 10 is shown

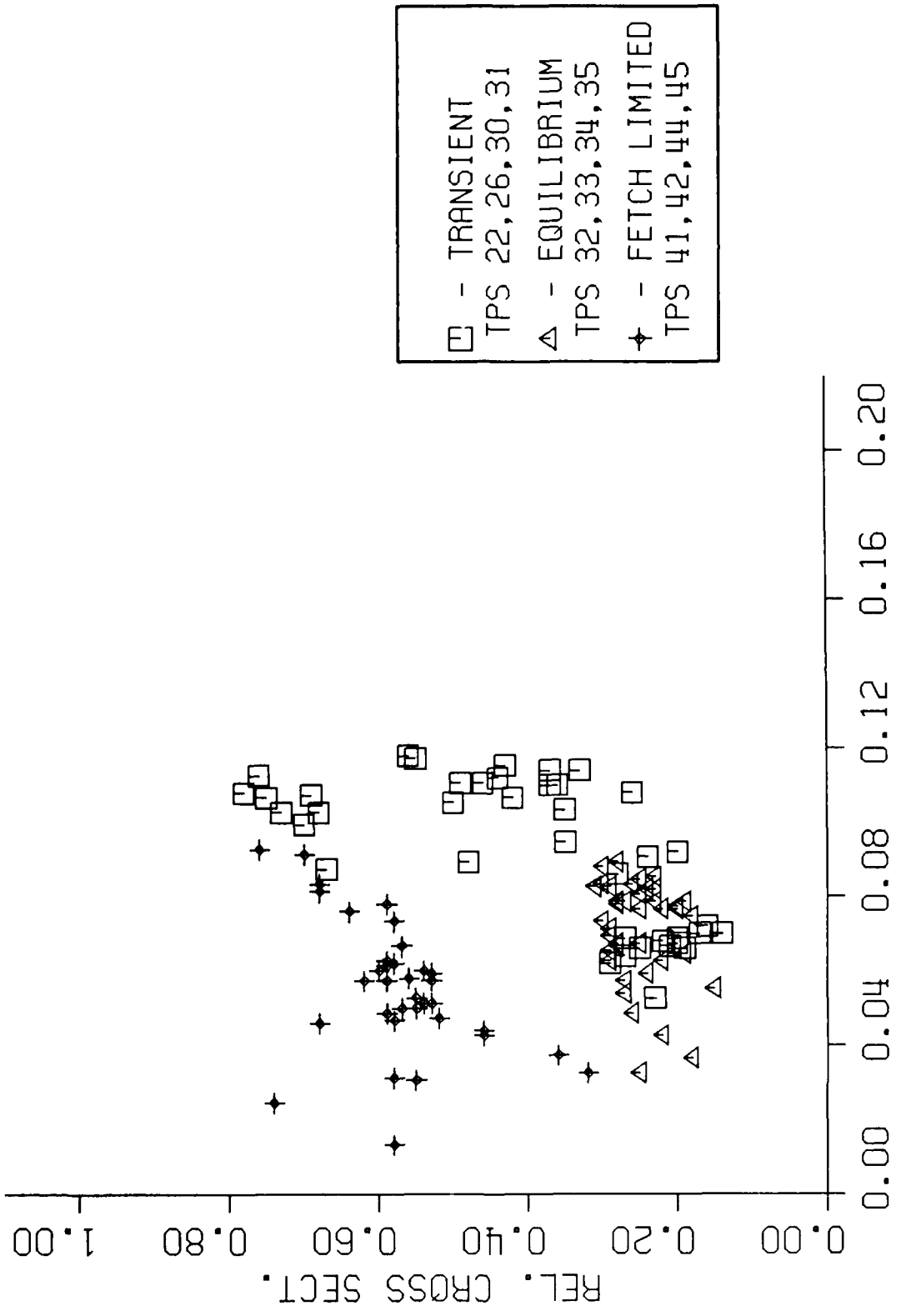


Fig. 13 — A plot of RCS vs $S_{loc3}$ defined in Eq. 11 is shown

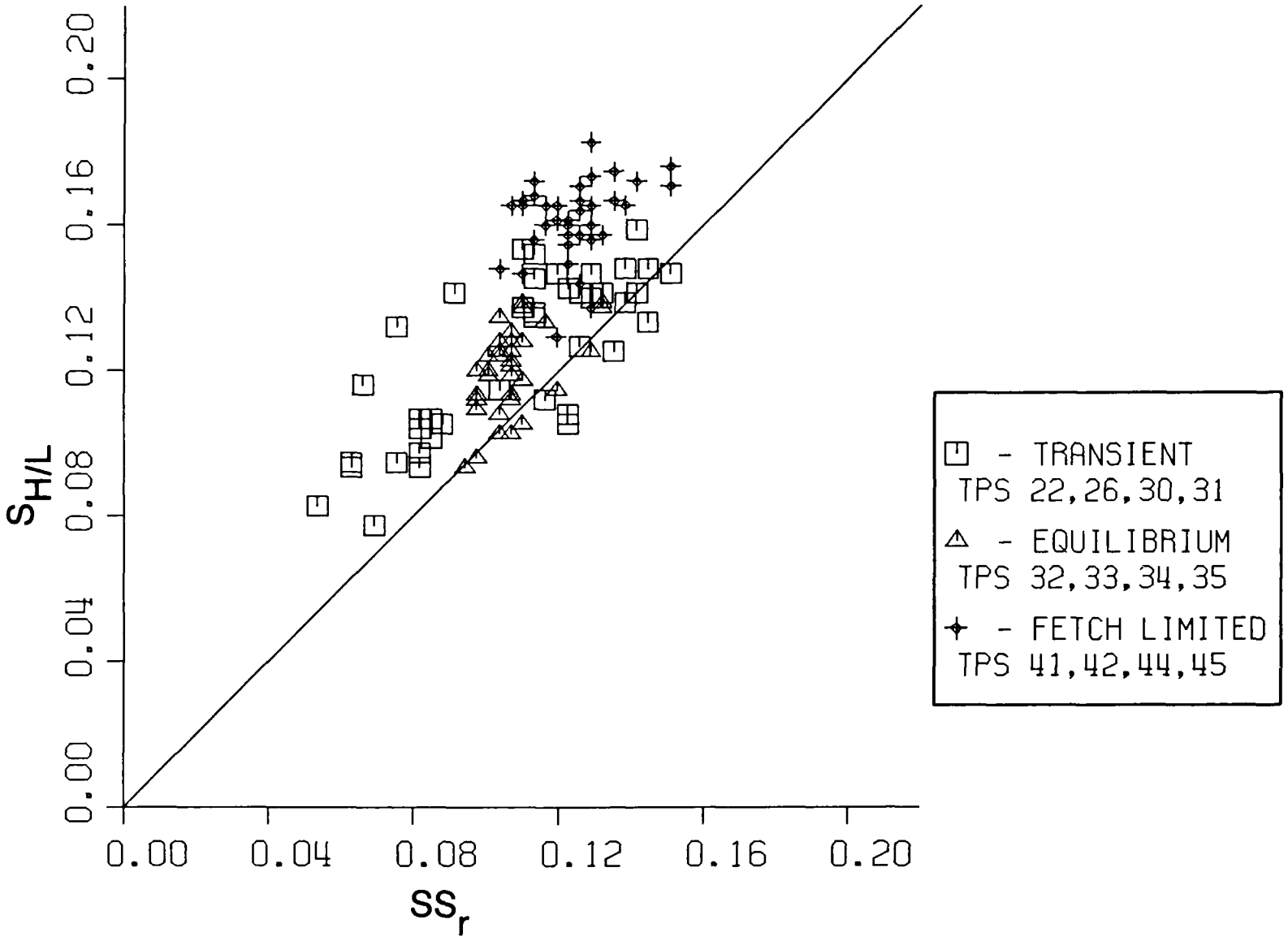


Fig. 14 — A plot of $S_r$ vs $S_{H/L}$ is shown, the scatter indicating the two being quite different measures of the surface

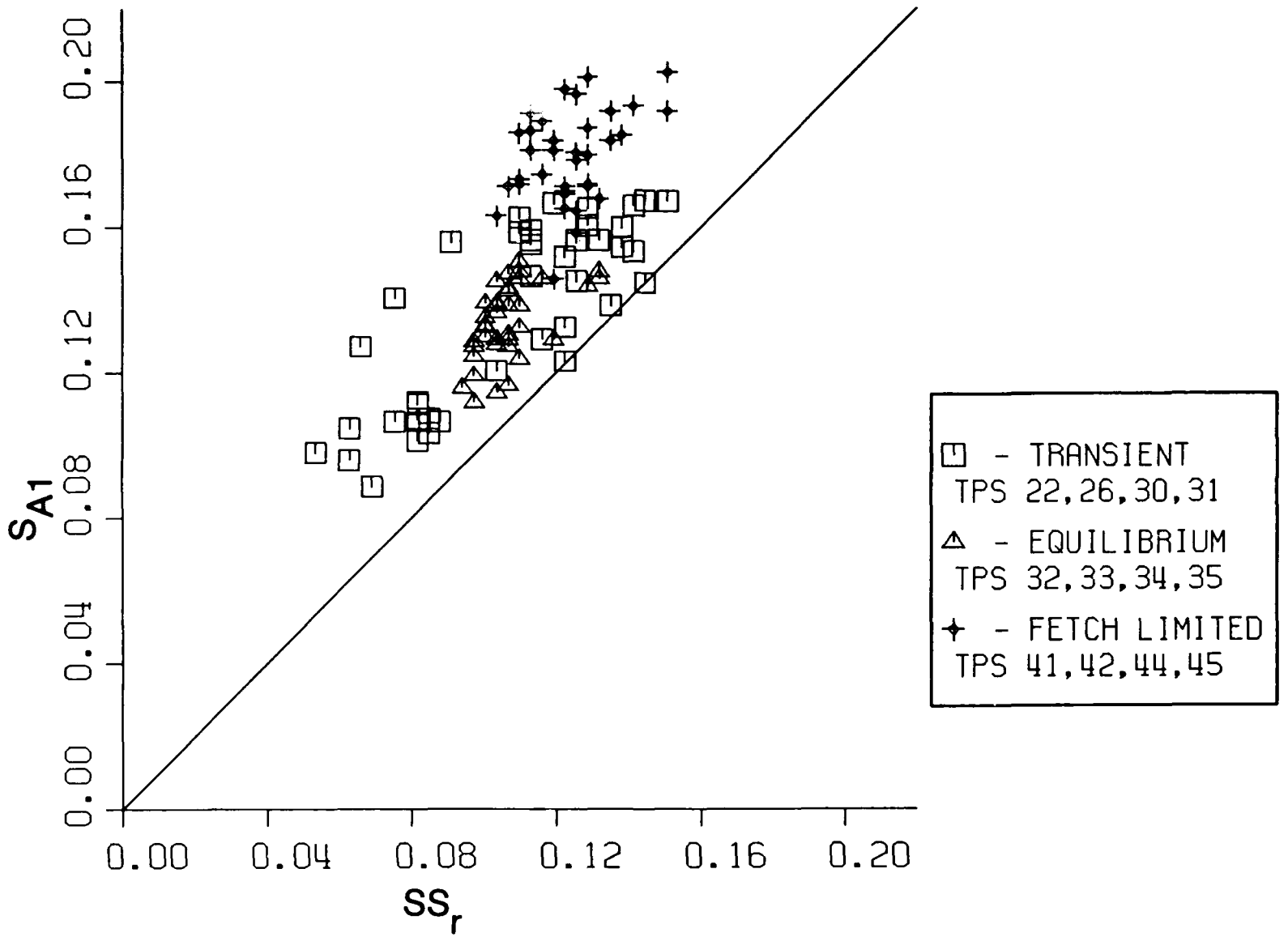


Fig. 15 — A plot of $S_r$ vs $S_{A1}$ is shown, which looks very similar to the previous plot

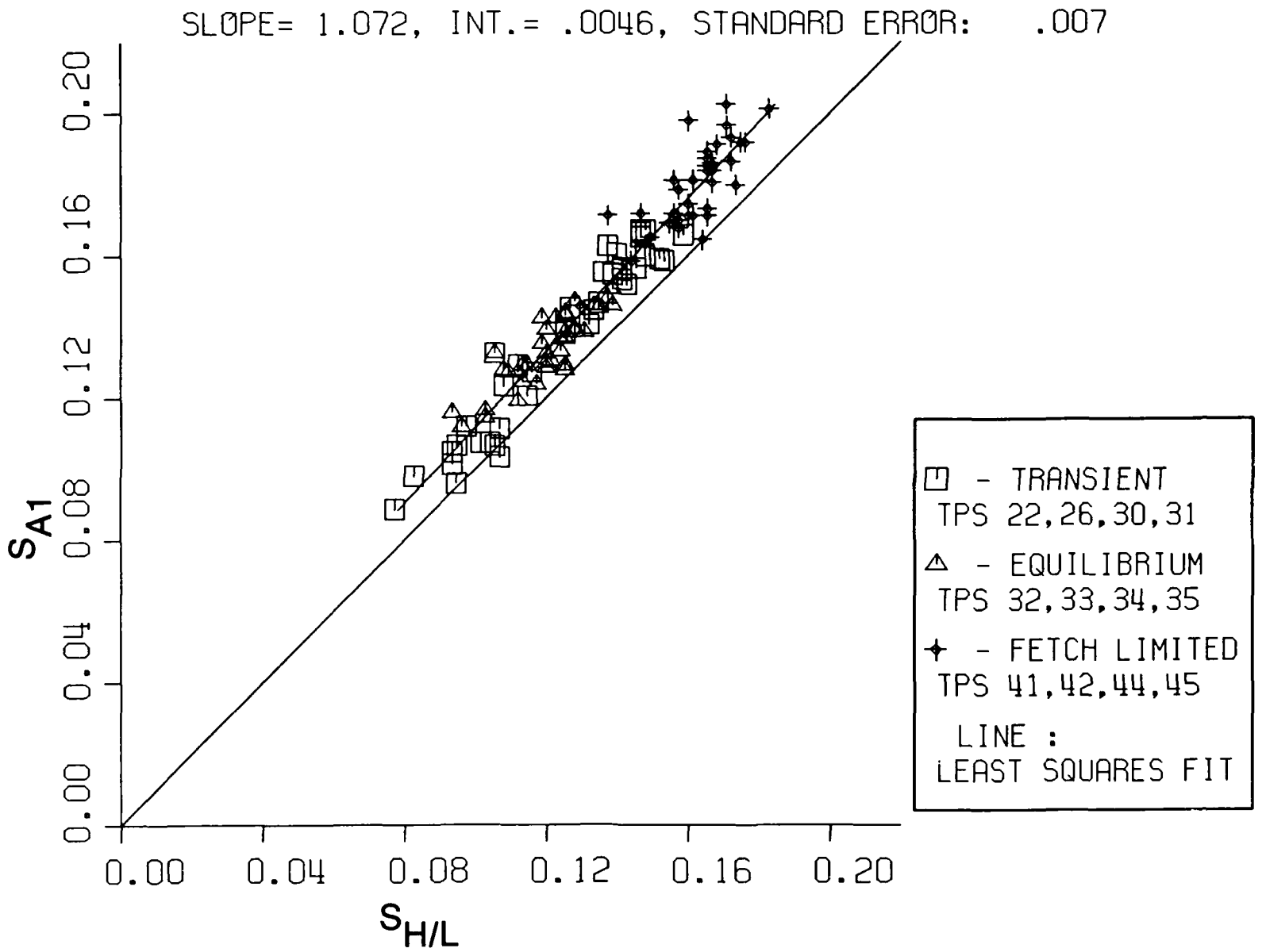


Fig. 16 — A scatter plot of $S_{A1}$ vs $S_{H/L}$ is shown, showing the increased steepness of the forward face slope compared to the sinusoidal approximation

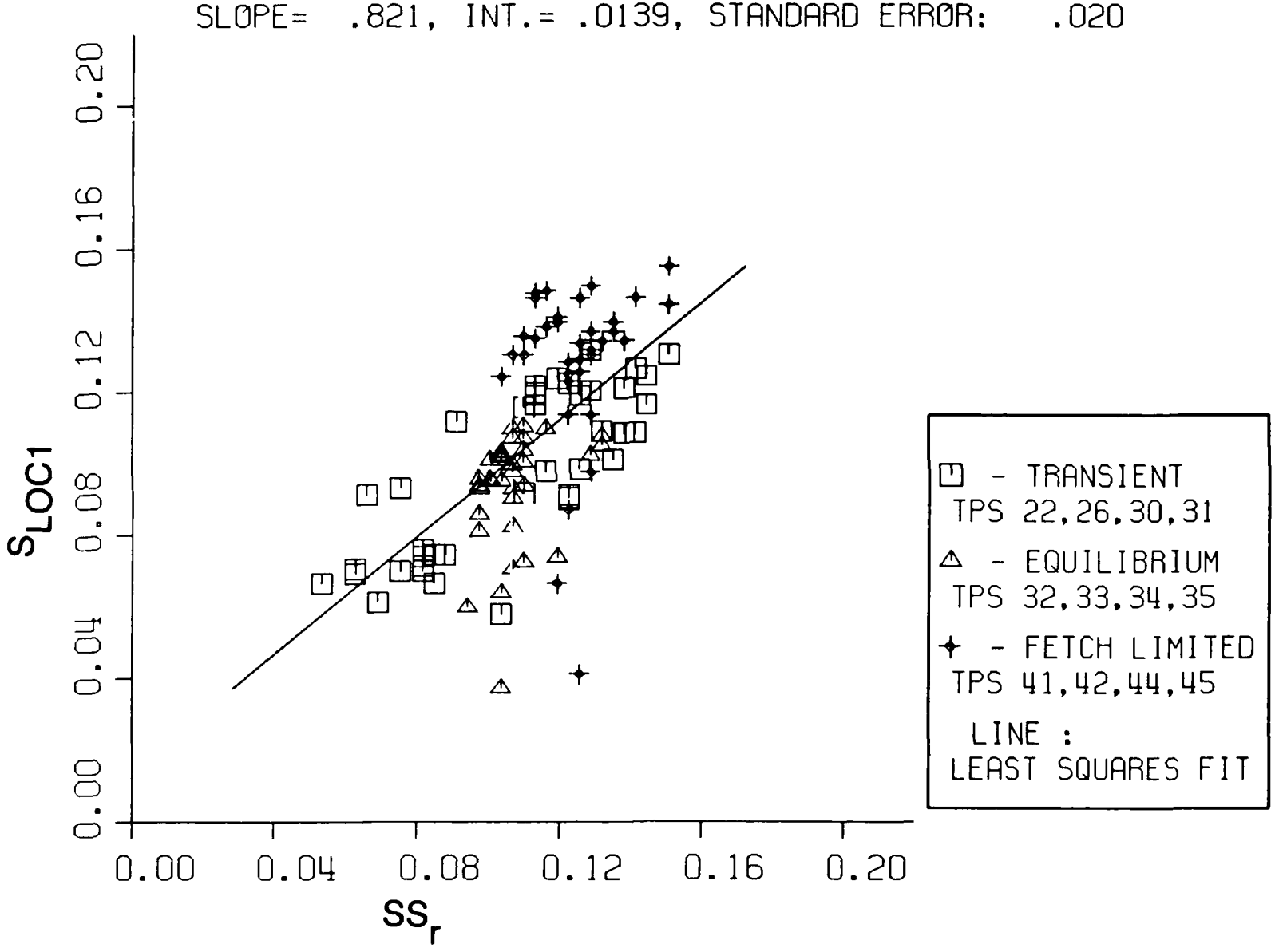


Fig. 17 — A plot of $S_r$ vs $S_{loc1}$ is shown, indicating rather poor correlation

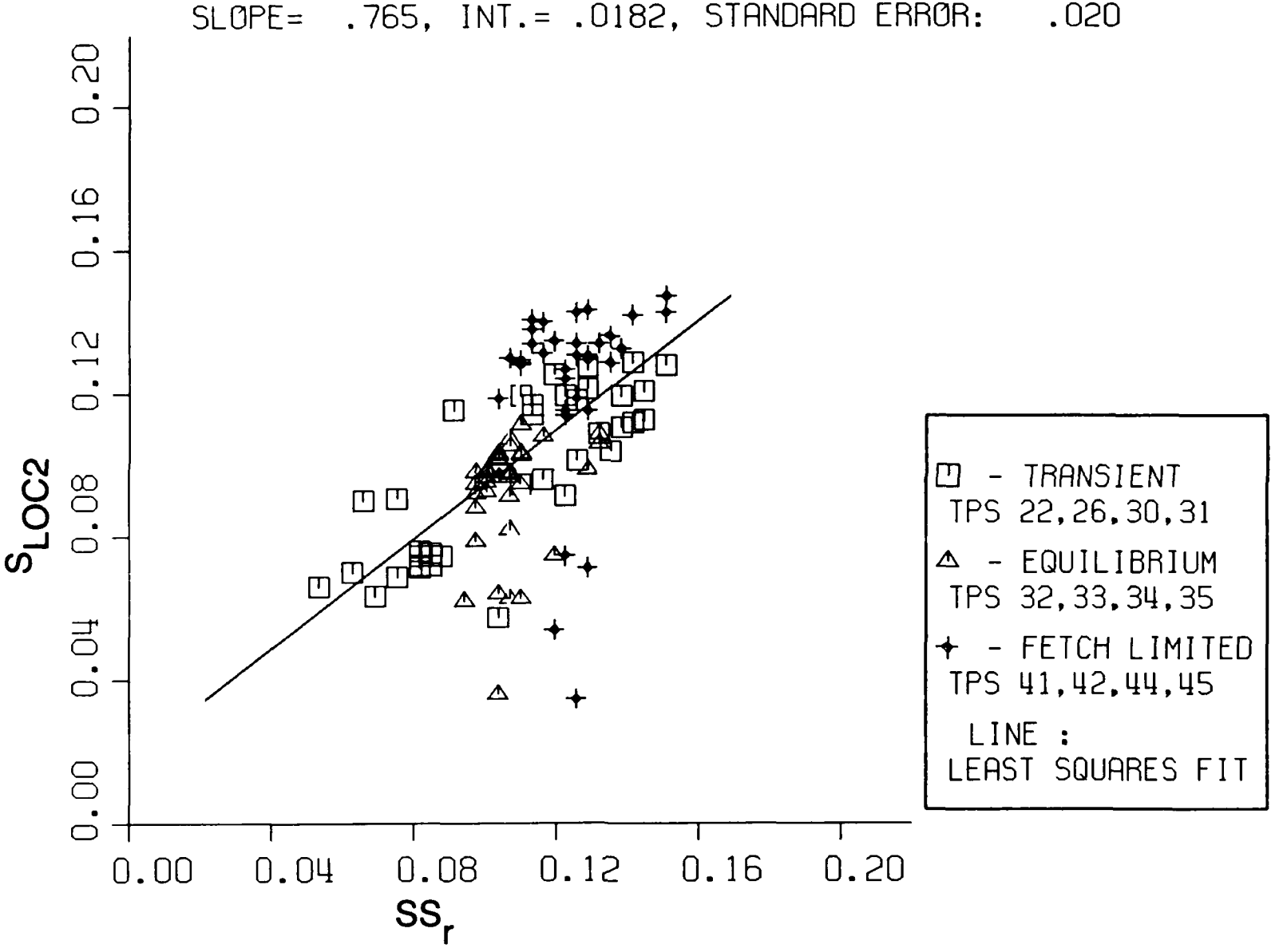


Fig. 18 — A plot of $S_r$ vs $S_{loc2}$ is shown, with results similar to the previous plot

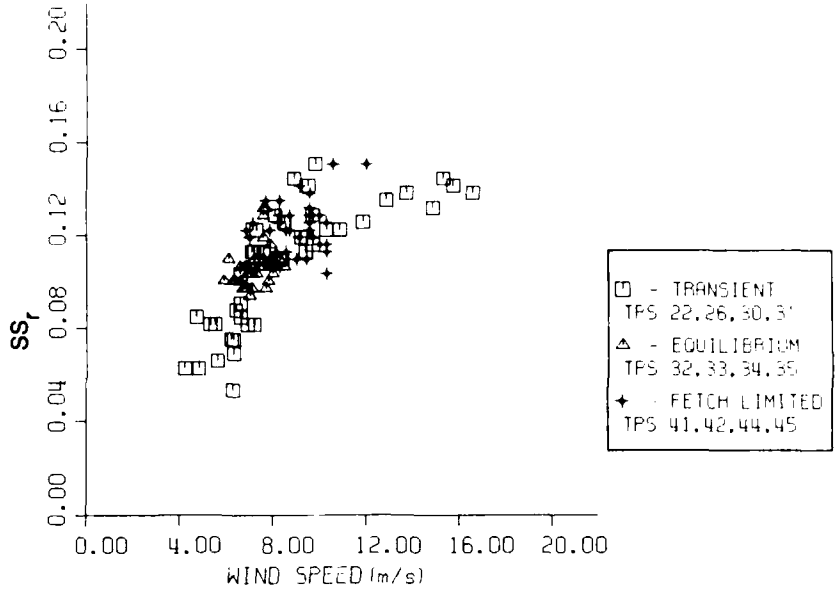


(a)

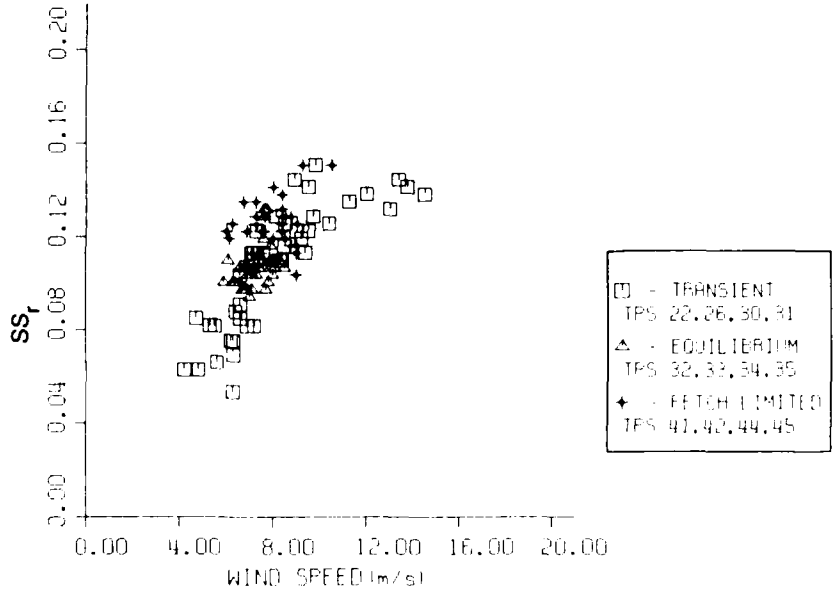


(b)

**Fig. 19 — Plots of radar slopes vs wind speed are shown, with wind speeds corrected for the fetch limited and the first transient data set. Corrections are for 30% (a), 20% (b), 10% (c), and uncorrected (d).**

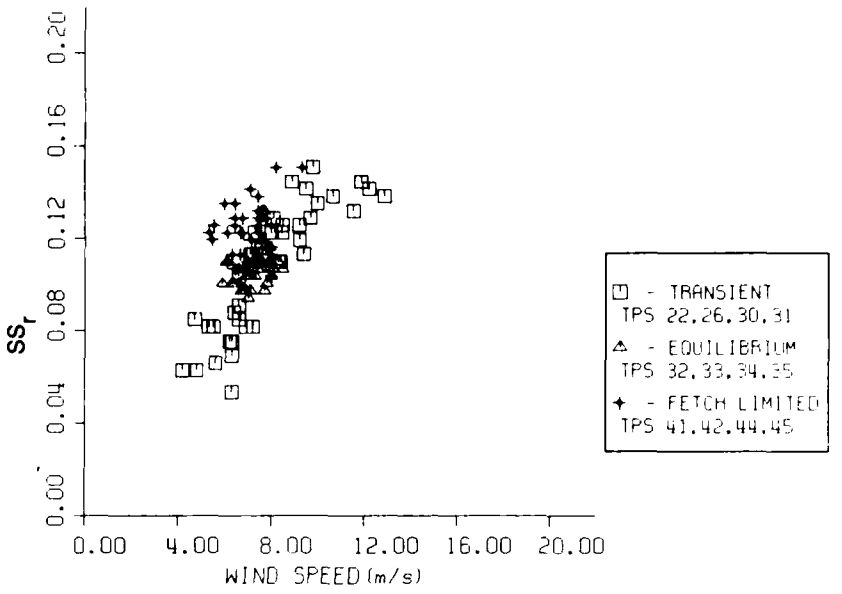


(c)

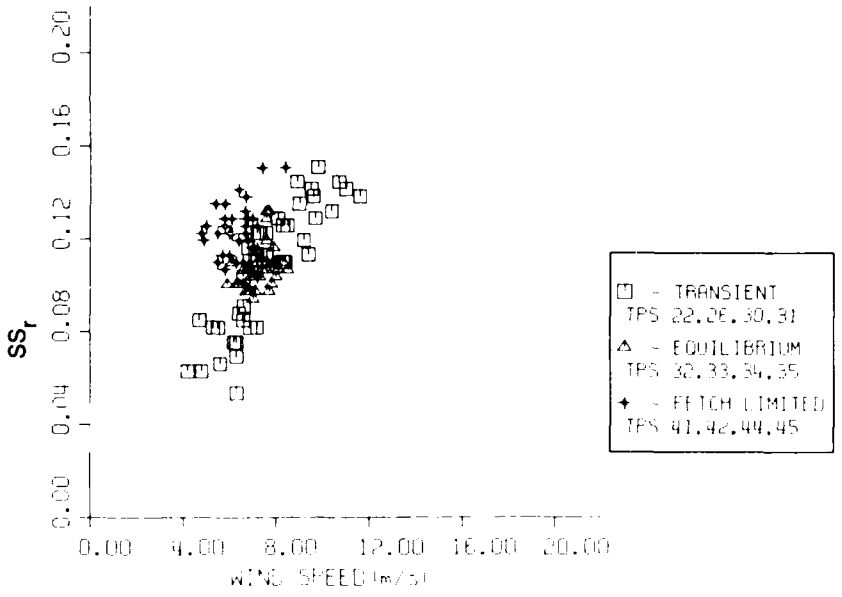


(d)

Fig. 19 (Continued) — Plots of radar slopes vs wind speed are shown, with wind speeds corrected for the fetch limited and the first transient data set. Corrections are for 30% (a), 20% (b), 10% (c), and uncorrected (d).

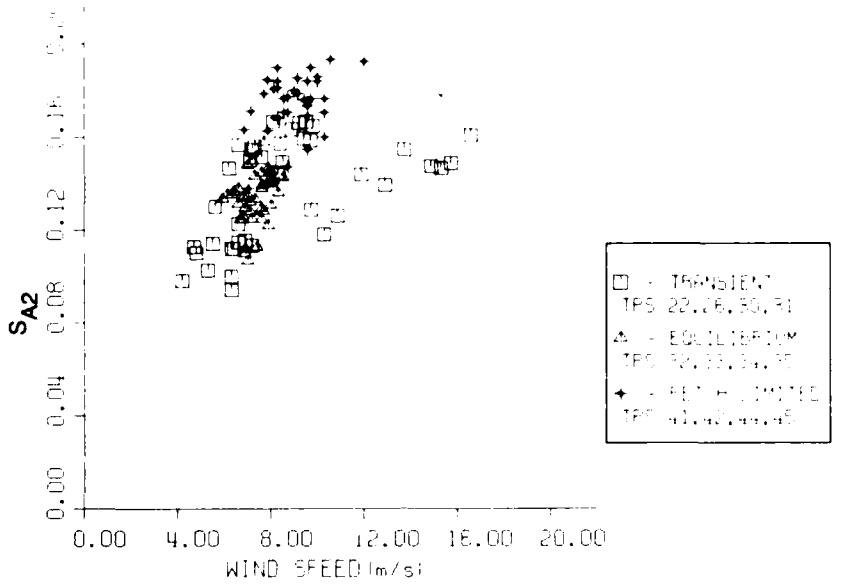


(a)

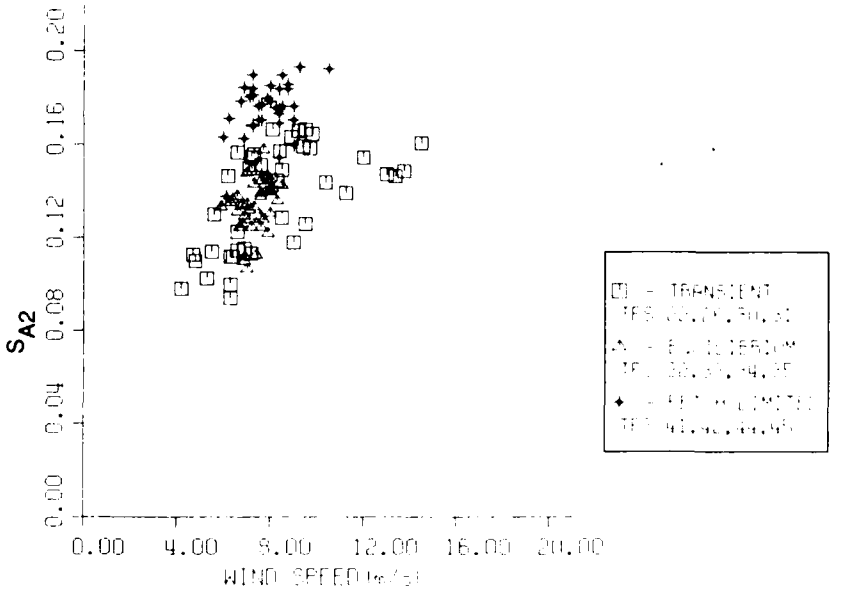


(b)

Fig. 20 — Plots of $S_{A1}$ vs wind speed are shown, with wind speeds corrected as for the previous figure: 30% (a), 20% (b), 10% (c) and uncorrected (d).

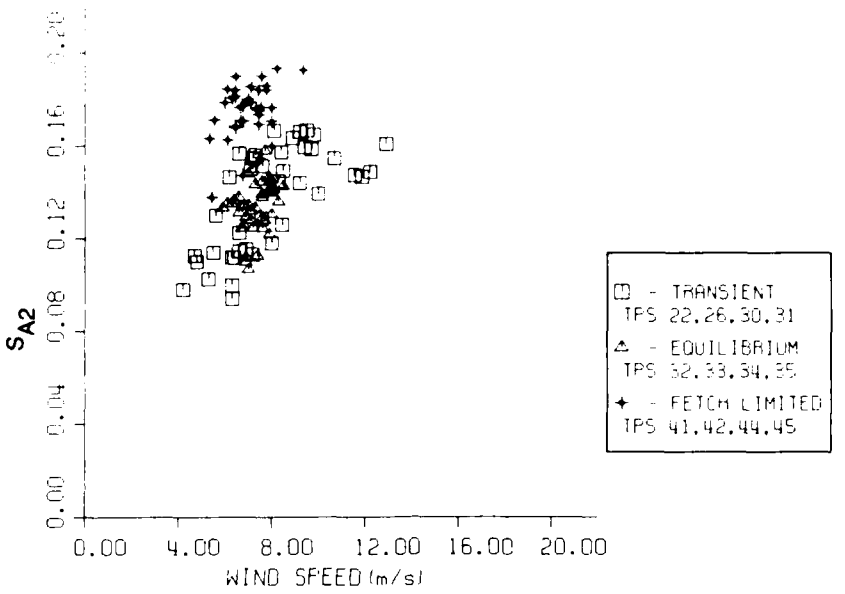


(c)

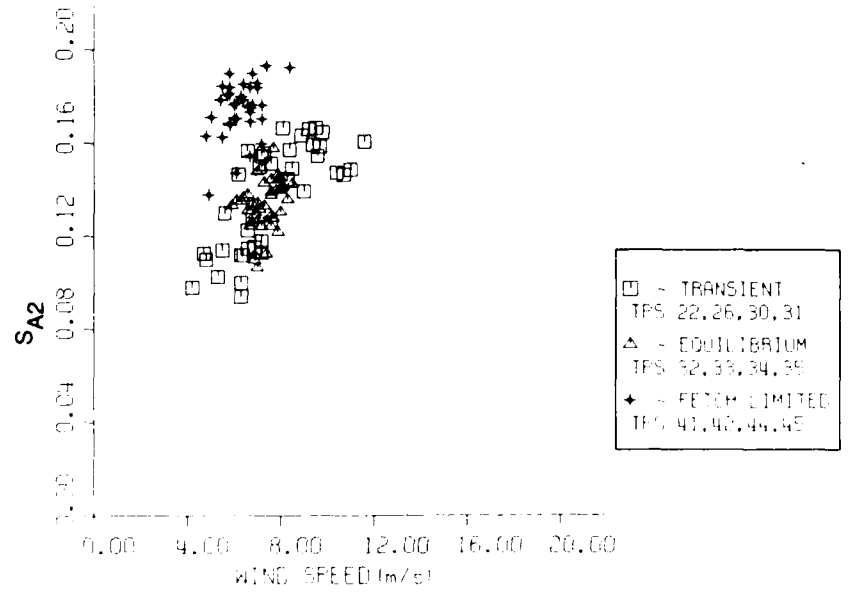


(d)

Fig. 20 (Continued) — Plots of $S_{A1}$ vs wind speed are shown, with wind speeds corrected as for the previous figure: 30% (a), 20% (b), 10% (c) and uncorrected (d).

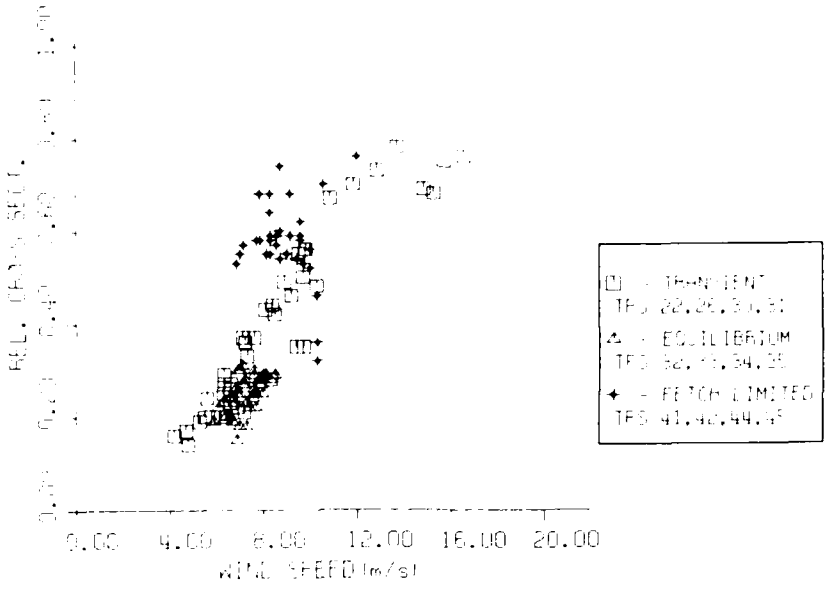


(a)

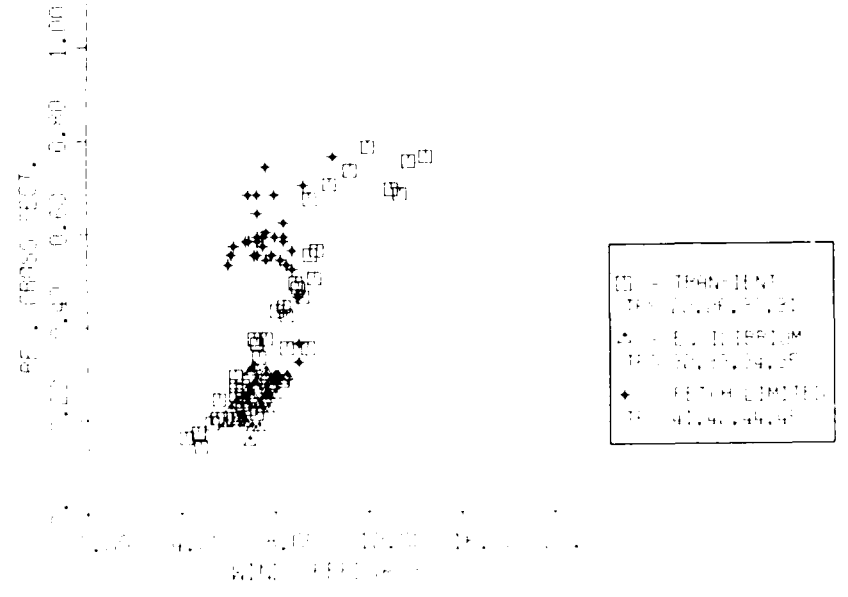

(b)

Fig. 21 — Plots of relative cross section vs wind speed, with wind speeds corrected as before: 30% (a), 20% (b), 10% (c) and uncorrected (d).

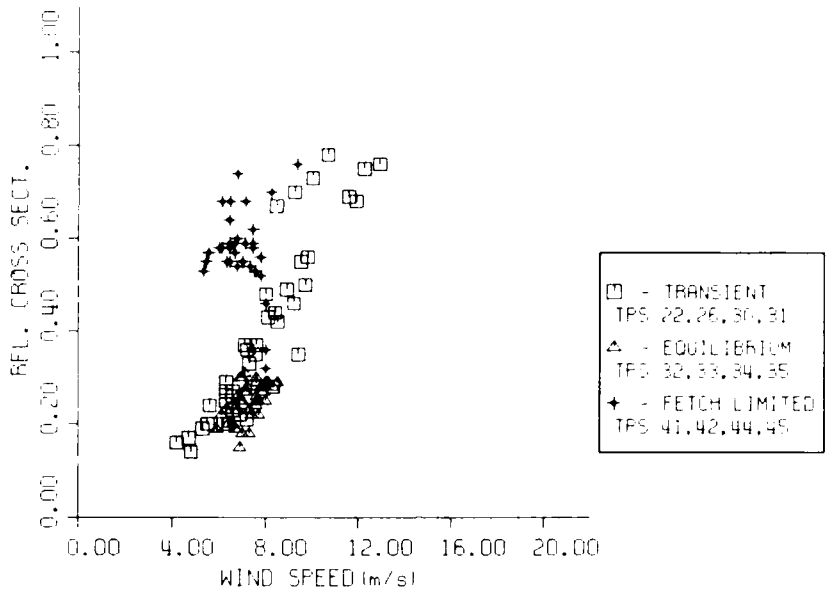


(c)

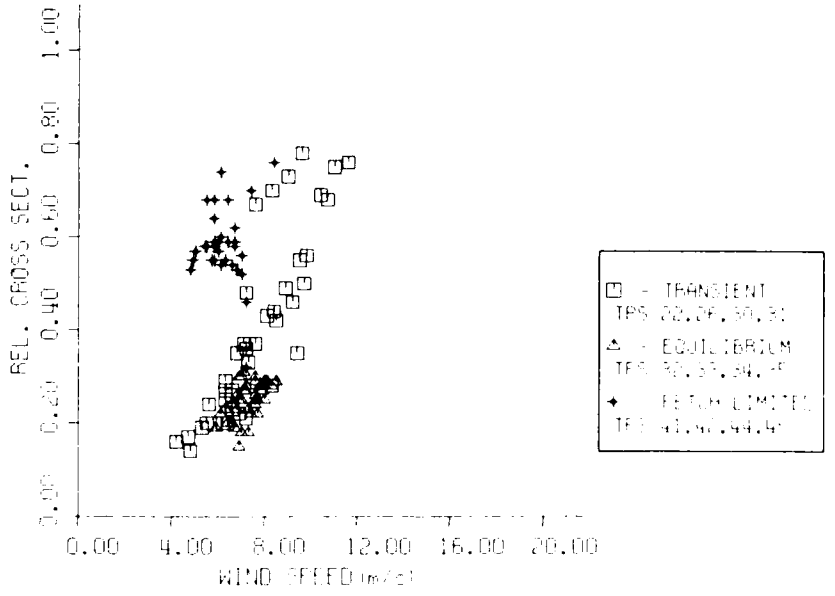


(d)

Fig. 21 (Continued) — Plots of relative cross section vs wind speed, with wind speeds corrected as before: 30% (a), 20% (b), 10% (c) and uncorrected (d).

END

DATE

FILMED

DTIC

JULY 88